Ind. J. Pharm. Edu. Res., 2026; 60(3):1131-1142.
https://www.ijper.org

Original Article

Anticancer Activity of *Angelica dahurica* Used in Traditional Chinese Medicine (TCM) against Human Breast Cancer Cells: Mechanistic Evaluation by Using an Integrated Approach of Network Pharmacology, Computational Molecular Docking and Experimental Assays

Yanqiu Li[1,#], Chenhui Zhao[2,#], Yanling Ren[3], Liping Xie[4,*]

[1]Department of Pharmacy Dispensing, The Fourth Affiliated Hospital of Harbin Medical University, Harbin, Heilongjiang, CHINA.
[2]Department of General Surgery, Chongqing Western Hospital, Chongqing, CHINA.
[3]Department of Physical and Chemical Inspection, Jinzhong Center for Disease Control and Prevention, Jinzhong, Shanxi, CHINA.
[4]Department of Pharmacy, Ningde Mindong Hospital affiliated to Fujian Medical University, Fuan, Fujian, CHINA.
[#]*Yanqiu Li and Chenhui Zhao are co-first authors, they contributed equally to this work.*

ABSTRACT

Background: Breast Cancer (BC) remains a major global health challenge, necessitating novel treatment approaches to improve therapeutic outcomes. *Angelica dahurica*, a traditional medicinal plant, contains phytochemicals with potential anticancer properties, offering a promising avenue for investigation. **Aim:** This study evaluates the anticancer potential of *Angelica dahurica* extract against BC by integrating *in silico* network pharmacology with *in vitro* experimental validation, focusing on the modulation of key oncogenic targets STAT3, SRC, and MAPK1. **Materials and Methods:** *In silico*, phytochemicals from *Angelica dahurica* were screened using the TCMSP database, with targets predicted via SwissTargetPrediction and SuperPred. BC-related targets from GeneCards were intersected using JVenn. A protein-protein interaction network was constructed with STRING, analyzed in Cytoscape, and key targets identified via cytoHubba. Molecular docking was performed using DockThor, and SRPlot assessed functional relevance. *In vitro*, MCF-7 (BC) and MCF-10 (normal) cell lines underwent MTT cytotoxicity, clonogenic, EdU proliferation, Annexin V/PI apoptosis, and Western blotting assays. **Results:** *In silico* screening filtered 99 phytochemicals to 13, yielding 155 unique targets based on OB≥30%, DL≥0.18, and Caco-2 filters. From 3,899 BC-related targets, 138 overlapped, with STAT3, SRC, and MAPK1 as central hubs. Docking confirmed sitogluside's strong binding to these targets, with high-affinity binding energies. SRPlot revealed enriched pathways in proliferation and apoptosis. *In vitro*, the extract showed dose-dependent cytotoxicity in MCF-7 cells (40-160 µg/mL), reducing viability by up to 60%, with minimal MCF-10 toxicity. Clonogenic assays indicated 70% inhibition of colony formation, and EdU assays showed 50% reduction in DNA synthesis. Annexin V/PI staining confirmed 40% apoptosis induction. Western blotting revealed dose-dependent downregulation of STAT3, SRC, and MAPK1, with reductions up to 65%. **Conclusion:** *Angelica dahurica* extract, particularly sitogluside, effectively targets key oncogenic pathways in breast cancer, supporting its potential as a novel therapeutic agent against BC.

Keywords: *Angelica dahurica*, Network-Pharmacology, Breast Cancer, Gene-ontology Enrichment Analysis, Molecular Docking, Cytotoxicity.

Correspondence:
Dr. Liping Xie
Department of Pharmacy, Ningde Mindong Hospital Affiliated to Fujian Medical University, Fuan, Fujian-355000, CHINA.
Email: xielp28970@outlook.com
ORCID: 0009-0005-1154-8527

Received: 16-10-2025;
Revised: 23-01-2026;
Accepted: 05-03-2026.

INTRODUCTION

BC is still among the most common cancers in women globally. In 2024, global estimates indicated that over 2.3 million BC cases were diagnosed annually, with more than 680,000 deaths attributed to the disease.[1] Despite advances in conventional therapies such as surgery, radiotherapy, and chemotherapy, challenges including drug resistance and adverse side effects necessitate the exploration of novel therapeutic strategies.[2] Natural products, and in particular Traditional Chinese Medicine (TCM), have gained considerable attention due to their multitarget activities and synergistic effects. TCM has been practiced for millennia, offering a holistic approach to disease management, and its compounds have recently emerged as promising leads in anticancer drug discovery.[3]

Angelica dahurica, commonly known as Baizhi in Traditional Chinese Medicine, has long been valued for its anti-inflammatory, pain-relieving, and detoxifying properties.[4]

DOI: 10.5530/ijper.20262481

Recent pharmacological examinations have unveiled that its bioactive components may exert antitumor effects, including the stimulation of apoptosis and the suppression of cell growth in different cancer cells.[5] The diverse phytochemical profile of *Angelica dahurica*-encompassing coumarins, volatile oils, and polysaccharides-provides a unique opportunity to explore its mechanistic role against breast cancer.[6]

Network pharmacology has emerged as an advanced approach to systematically explore the complex interactions between bioactive compounds and biological systems, addressing challenges in understanding their mechanisms.[7] By integrating bioinformatics with experimental validation, it enables researchers to identify potential targets, elucidate molecular pathways, and uncover synergistic effects often missed in traditional single-target studies. In the context of Traditional Chinese Medicine (TCM), where herbal medicines involve multiple compounds acting on various pathways, this approach is particularly valuable.[8] It provides a framework to bridge empirical evidence with molecular mechanisms, enhancing the clinical relevance of TCM-based interventions.

Angelica dahurica multifaceted pharmacological profile offers promising avenues for its use as an anticancer agent. Previous studies have suggested that its compounds might interact with key regulatory proteins involved in cell proliferation, apoptosis, and metastasis.[9,10] Yet, a systematic study combining network pharmacology with *in vitro* validation is necessary to significantly define these interactions.

The integration of computational predictions with experimental validation has not only accelerated drug discovery but also improved our understanding of the mechanistic interplay between natural compounds and cancer biology. This investigation leverages a series of online databases and bioinformatics tools-including the TCMSP (http://tcmsp-e.com/tcmsp.php), SwissTargetPrediction (https://www.swisstargetprediction.ch/),[11] SuperPred (https://prediction.charite.de/), GeneCards (https://www.genecards.org/),[12] Jvenn (https://jvenn.toulouse.inrae.fr/), STRING (https://string-db.org/),[13] SRPlot (https://www.bioinformatics.com.cn/en), and DOCKTHOR (https://dockthor.lncc.br/v2/)[14] to systematically profile the phytochemicals present in *Angelica dahurica*, predict their molecular targets, and elucidate the potential pathways implicated in breast cancer therapy. These digital resources have been instrumental in enhancing the precision and reproducibility of target identification, allowing for the integration of vast datasets into a coherent pharmacological network. Furthermore, we utilize an integrated experimental approach comprising phytochemical screening, target identification, Protein-Protein Interaction (PPI) network construction, and pathway enrichment analysis, followed by molecular docking to assess binding affinities. This theoretical framework is supported by a range of cell-based assays, including MTT cytotoxicity, colony formation, EdU proliferation, Annexin V/PI apoptosis, and Western blotting, to experimentally validate the identified hub genes and elucidate their role in the biological activity of the herbal extract (Supplementary Figure 1).

MATERIALS AND METHODS

Phytochemical Screening

The preliminary screening of phytochemicals from *Angelica dahurica* was performed using the TCMSP database. This platform, which offers extensive information on the Absorption, Distribution, Metabolism, and Excretion (ADME) properties of TCM compounds, was employed with stringent filters: oral bioavailability (OB) ≥ 20%, Drug-Likeness (DL)≥0.18, and Caco-2 cell permeability criteria.[15] Caco-2 cell permeability, measured using a human colon carcinoma cell line that mimics the small intestine's epithelial lining, predicts intestinal absorption and oral bioavailability by assessing a compound's ability to cross a polarized monolayer, expressed as the apparent permeability coefficient (Papp, cm/s).

By applying these filters, we curated a subset of compounds with high drug likeness potential.

Target Selection

The selected phytochemicals were then subjected to target prediction using two online platforms: SwissTargetPrediction and SuperPred. Inputting the molecular structures into these platforms generated a list of probable protein targets based on chemical similarity and pharmacophore mapping. A probability filter (≥0.75) was applied to ensure high confidence in the predicted targets. Disease-related targets were further refined using the GeneCards database by cross-referencing known breast cancer-associated genes. This integrative approach provided a significant list of candidate targets for subsequent analysis.

PPI Network Generation

Common targets identified from both the compound prediction and disease databases were then visualized using the Jvenn online platform, which facilitated the intersection analysis between the two datasets. The intersecting genes were subsequently entered into the STRING database for PPI (Protein-Protein Interaction) network construction, with a minimum confidence score set at 0.400 to include only reliable interactions. The resulting PPI network was exported and further analyzed using Cytoscape software (v3.10.2). Within Cytoscape, the Cytohubba plugin was applied to identify hub genes based on degree method that are central to the network and potentially critical in modulating effectiveness of *Angelica dahurica* in BC.

Functional Enrichment

The GO and KEGG pathway analyses were accomplished using the SRPlot tool. These analyses enabled the identification of biological processes, molecular functions, and pathways

significantly allied with the predicted targets, thereby providing insight into the mechanisms underlying the herb's anticancer activity.

Molecular Docking

Molecular docking studies were conducted using the DOCKTHOR online tool to evaluate the binding affinity between a top-scoring molecule, Sitogluside, and three key hub proteins: STAT3, SRC, and MAPK1. Protein structures were downloaded from the RCSB-PDB database STAT3 (6nuq), SRC (1yog), and MAPK1 (6nyb) and prepared using Discovery Studio (Dassault Systèmes, Waltham, MA 02451, USA).[16-18] Water molecules were eliminated and missing hydrogen atoms were added using this software. The ligand structure was designed and optimized using ChemDraw (PerkinElmer, Waltham, MA 02451, USA). Docking simulations were performed with flexible parameters for both the ligand and the binding site, ensuring accurate predictions of the interaction energies and binding modes.

Plant Material Extraction

The aerial parts of *Angelica dahurica* were collected, authenticated, and air-dried. The dried material was ground into a fine powder. Soxhlet extraction was then performed using 95% ethanol as the solvent. Approximately 50 g of the powdered plant material was placed in a Soxhlet extractor and refluxed continuously for 3 hr. The extraction was carried out at 78°C, and under decreased pressure, the rotary evaporator was used to concentrate the resultant extract.

Chemicals, Reagents and Equipment

The chemicals and reagents used in the experimental procedures were procured from reputable suppliers. Ethanol (analytical grade) was sourced from Merck (Merck KGaA, Frankfurter Strasse 250, 64293 Darmstadt, Germany). The MTT reagent was obtained from Sigma-Aldrich (Sigma-Aldrich Corporation, 3050 Spruce Street, St. Louis, MO 63103, USA). Cell culture media and supplements were provided by Gibco (Thermo Fisher Scientific, 168 Third Avenue, Waltham, MA 02451, USA). The BioTek ELx800 microplate-reader (BioTek-Instruments, VT 05404, United States) was used to read absorbance. Antibodies used for western blotting, including anti-STAT3, anti-SRC, anti-MAPK1, and HRP-conjugated secondary antibodies, were purchased from Santa Cruz Biotechnology (2701 N. Meridian Blvd, Dallas, TX 75204, USA). The microscopes used were the Nikon Eclipse 80i Microscope (Nikon Corporation, 5-7-1 Shiba, Minato-ku, Tokyo, Japan) and the Carl Zeiss LSM 710 Confocal Microscope (Oberkochen, Germany).

Cell Lines and Culture Conditions

Normal mammary epithelial cells (MCF-10) and breast cancer cells (MCF-7) were obtained from the American Type Culture Collection (ATCC). Cells were cultured in Dulbecco's Modified Eagle's Medium (DMEM) supplemented with 10% Fetal Bovine Serum (FBS), 100 U/mL penicillin, and 100 µg/mL streptomycin at 37°C in a humidified atmosphere containing 5% CO_2.

MTT Cytotoxicity Assay

The cytotoxic efficiency for *Angelica dahurica* extract was estimated using the MTT assay. Cells were seeded in 96-well plates at a density of 5×10^3 cells per well and allowed to adhere overnight. The extract was then added at concentrations of 0, 20, 40, 80, and 160 µg/mL. After 24 hr of treatment, 20 µL of MTT solution (5 mg/mL in PBS) was added to each well, followed by a further 4 hr of incubation for the plates. The microplate reader measured the absorbance at 570 nm after the formazan crystals were dissolved in 150 µL of DMSO.

Clonogenic Assay

To assess the long-term proliferation and survival in MCF-7 cells, a clonogenic assay was performed. Cells were plated in 6-well plates at low density and treated with the extract at 0, 40, 80, and 160 µg/mL for 24 hr. After treatment, cells were allowed to grow in fresh medium for 14 days. Colonies were fixed with methanol, stained with crystal violet, and imaged using the Nikon Eclipse 80i microscope. Colony counts were done manually, and survival percentages were computed.

EdU Proliferation Assay

To evaluate and quantify MCF-7 cell-proliferation, the EdU test was used. The EdU (5-ethynyl-2'-deoxyuridine) assay measures cell proliferation by detecting DNA synthesis, incorporating EdU, a thymidine analog, into newly synthesized DNA during the S-phase, which is then fluorescently labeled via click chemistry for visualization and quantification using fluorescence microscopy or flow cytometry. Following treatment with 0, 40, 80, and 160 µg/mL of the extract for 24 hr, cells were incubated with EdU for 2 hr. The incorporated EdU was detected using a fluorescent azide according to manufacturer's provided protocol. Fluorescent images were taken with the Carl Zeiss LSM 710 confocal microscope, and the number of cells that took up EdU was measured.

Apoptosis Analysis

DAPI staining: MCF-7 cells were seeded in culture plates and, upon reaching optimal confluence, were subjected to treatment with *Angelica dahurica* extract at various concentrations. Following a 24-hr incubation, the cells were washed with PBS and fixed using 4% paraformaldehyde for 15 min at room temperature to preserve cellular morphology. After fixation, cells were permeabilized with 0.1% Triton X-100 and subsequently incubated with DAPI solution (1 µg/mL) for 10 min in the dark. The staining process allowed for selective binding of DAPI to A-T rich regions of the DNA, enabling the visualization of nuclear morphology under a fluorescence microscope. This experimental setup was designed

to assess apoptotic changes by highlighting nuclear condensation, fragmentation, and other morphological alterations indicative of cell death.

Annexin V/PI Apoptosis Assay: Apoptotic cell death was quantified using Annexin V-FITC/PI staining. MCF-7 cells were treated with the extract at 0, 40, 80, and 160 µg/mL for 24 hr. Cells were then harvested, washed with cold PBS, and resuspended in binding buffer. Annexin V-FITC and PI were added, and samples were incubated in the dark for 15 min at room temperature. Apoptotic cells were analyzed by flow cytometry, and selected fields were imaged using the Nikon Eclipse 80i microscope.

Western Blotting

To validate the expression of hub genes identified through network pharmacology, Western blot analysis was performed. Protein extracts from treated and protease inhibitor-supplemented RIPA buffer were used to prepare untreated MCF-7 cells. After subjecting the proteins to SDS-PAGE separation, the same quantities were transferred to PVDF membranes. Primer antibodies targeting STAT3, SRC, and MAPK1 (1:1000 dilution) were applied to the membranes after blocking with 5% nonfat milk in TBST. The membranes were then left to incubate overnight at 4°C. Densitometry software (ImageJ Software; Version 1.54m) was used to measure the visible bands after they were treated with HRP-conjugated secondary antibodies (1:5000 dilution).

Data Analysis

All experiments were conducted in triplicate, and findings are expressed as mean ± standard deviation. Statistical significance was assessed using one-way ANOVA, followed by post hoc testing, with $*p<0.05$, $*p<0.01$ and $*p<0.001$ being statistically significant. We combined the computer predictions with the experimental results by comparing the molecular docking scores to the changes in hub gene expression measured by Western blotting and cell tests.

RESULTS

Phytochemical Screening and Target Prediction

An initial search of the TCMSP database identified 99 phytochemicals in *Angelica dahurica*. Application of screening criteria- OB≥30%, DL≥0.18, and Caco-2 cell permeability-reduced this list to 13 compounds (Supplementary Table 1). These 13 compounds were then subjected to target prediction using SwissTargetPrediction and SuperPred. By applying a probability threshold of 75% across the two platforms and consolidating duplicate entries, a final set of 155 unique targets was obtained (Supplementary Table 2). In parallel, breast cancer-related targets were retrieved from GeneCards by filtering with a GIFtS score of ≥ 55%. The GeneCards Inferred Functionality Score (GIFtS) quantifies the level of functional annotation for a gene in the GeneCards database, reflecting the extent of knowledge about its functionality. This initial screening yielded 50,000 potential targets, which were narrowed down to 3,899 targets of relevance (Supplementary Table 3). The integration of both phytochemical and disease-specific target profiles established a significant basis for subsequent analyses.

PPI Construction and Hub Gene Identification

The intersection between the 155 phytochemical-related targets and the breast cancer targets (identified from GeneCards) was determined using JVenn, revealing 138 common targets (Figure 1A). These intersecting targets were imported into the STRING database with parameters set for *Homo sapiens* to construct a comprehensive PPI network. Analysis within Cytoscape revealed a network composed of 114 nodes and 293 edges, demonstrating significant connectivity among the targets (Figure 1B). Further analysis using the cytoHubba plugin identified the top 10 hub genes: STAT3, SRC, MAPK1, HSP90AB1, MTOR, HIF1A, NFKB1, JAK2, PIK3CA, and PIK3R1 (Figure 1B), which are potentially crucial in mediating the biological activities of the phytochemicals in a breast cancer context.

Enriched Pathways

The shared targets were further examined through SRPlot online tools to determine their functional and biological relevance (Figure 1C). BP: Enrichment analysis highlighted processes such as peptidyl-serine phosphorylation, response to xenobiotic stimulus, cellular responses to peptides and alcohol, regulation of membrane potential, protein autophosphorylation, and neuron death regulation. CC: Significant terms included glutamatergic synapse, synaptic membrane structures (e.g., membrane raft, microdomain, presynaptic membrane), and specific synaptic specializations. MF: Key functions identified comprised protein serine/threonine kinase activity, phosphoric ester hydrolase activity, p53 binding, DNA-binding transcription factor activity, and histone kinase activity, in addition to neurotransmitter receptor activity. Enriched pathway analysis revealed several signaling routes and biological processes, including: Chemical carcinogenesis via receptor activation, Insulin resistance, EGFR-tyrosine-kinase-inhibitor-resistance, Sphingolipid signalling, Pancreatic cancer, Neurotrophin signaling pathway, Acute-myeloid-leukemia, Chemical carcinogenesis mediated by reactive oxygen species, Prolactin signaling, and pathways related to PD-L1 and PD-1 in cancer (Figure 2A). A combined network for the plant-compounds-targets-pathways was generated to signify the involvement of these compounds in different cellular pathways (Supplementary Figure 2). These conclusions deliver comprehension into the possible mechanisms by which the phytochemicals might exert their anticancer effects.

Molecular Docking Analysis

Using DockThor, docking examinations were conducted to assess the binding capability of phytochemicals produced from plants

against important cancer targets. Among the 13 compounds, Sitogluside emerged as the lead candidate. It demonstrated significant docking scores and molecular interactions with the top three hub proteins-STAT3, SRC, and MAPK1 (Supplementary Table 4 and Figure 2B). These interactions suggest that Sitogluside may effectively modulate pathways critical for tumor progression and may be worth exploring further in terms of experimental verification in breast cancer therapeutics.

MTT Cytotoxicity Assay

Treatment with the *Angelica dahurica* extract resulted in a clear, dose-dependent decrease in cell viability. In MCF-7 cells, significant cytotoxicity was detected starting from 40 µg/mL, with progressively lower absorbance values (and hence cell viability) recorded at 80 µg/mL and 160 µg/mL compared to untreated controls (Figure 3A). The IC_{50} value was found to be 75.2 µg/mL. MCF-10 cells demonstrated a more moderate response, indicating selective toxicity toward the cancerous phenotype.

Clonogenic Assay

Short-term exposure (24 hr) to the extract produced a significant, dose-dependent reduction in the long-term clonogenic survival of MCF-7 cells. Post-treatment incubation for 14 days revealed a marked decrease in the number and size of colonies (Figure 3B). At 160 µg/mL, the colony formation was substantially inhibited, with survival fractions significantly lower than the control group, indicating strong anti-proliferative effects (Figure 3C).

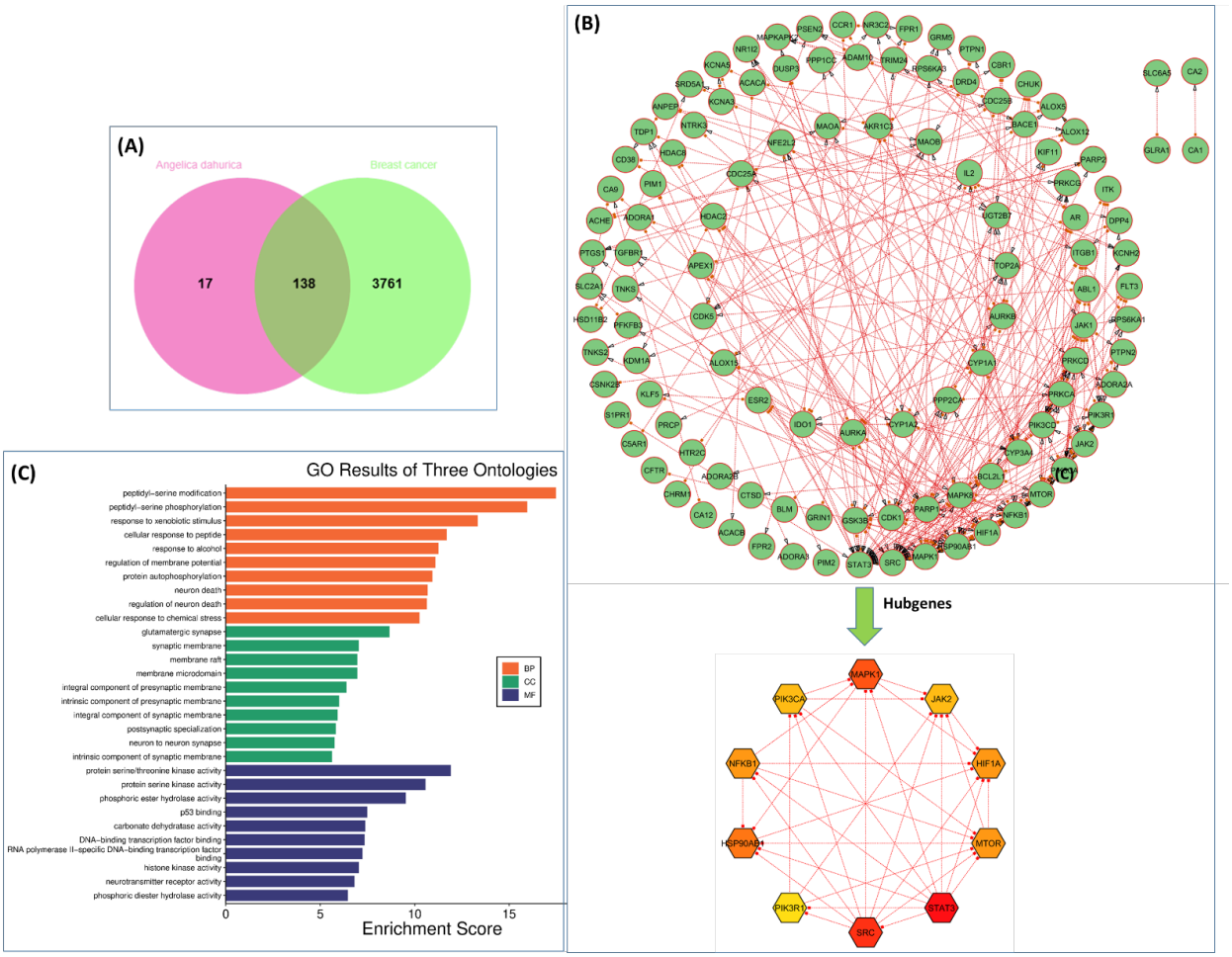

Figure 1: (A) Venn Diagram of Common Targets: Venn diagram generated using JVenn illustrating the intersection between 155 phytochemical-related targets and breast cancer targets sourced from GeneCards. The diagram shows that 138 common targets were identified, establishing the basis for subsequent network analyses. (B) Protein-Protein Interaction (PPI) Network Visualization: PPI network of the 138 common targets constructed using the STRING database (parameters set for Homo sapiens) and visualized in Cytoscape. This network comprises 114 nodes and 293 edges, reflecting extensive connectivity and the potential functional interplay among the targets. Hub Gene Analysis via cytoHubba: Network analysis using the cytoHubba plugin, highlighting the top 10 hub genes (STAT3, SRC, MAPK1, HSP90AB1, MTOR, HIF1A, NFKB1, JAK2, PIK3CA, and PIK3R1) within the PPI network. These hub genes are posited to play critical roles in the biological activities mediated by the phytochemicals in a breast cancer context. (C) GO Analysis: Graphical representation of GO enrichment analysis performed using SRPlot online tools. Panels depict results for BP, CC, and MF, with significant enrichment in processes such as peptidyl-serine phosphorylation, synaptic membrane architecture, and protein kinase activities.

Apoptosis induction

MCF-7 cells treated with 0- 160 µg/mL of the extract for 24 hr were processed for apoptosis detection. Flow cytometric data revealed a dose-dependent increase in early- and late-apoptotic cells, with significant elevation in Annexin V-positive cells at 80 and 160 µg/mL (Figures 3D and E). The DAPI assay results clearly revealed pronounced nuclear alterations in treated MCF-7 cells compared to control group. Cells exposed to increasing concentrations of the extract exhibited significant chromatin condensation and nuclear fragmentation, indicated by bright, punctate fluorescence patterns (Figure 4A). The intensity and pattern of DAPI fluorescence provided compelling visual evidence supporting the cytotoxic effects observed in the *in vitro* assays, thereby contributing to the overall understanding of the extract's anti-proliferative mechanism. These nuclear abnormalities corroborated the apoptosis detected through Annexin V/PI staining, reinforcing the conclusion that the *Angelica dahurica* extract effectively induces apoptosis.

EdU Proliferation Assay

In the EdU incorporation assay, a significant reduction in DNA synthesis was observed in MCF-7 cells following extract treatment. Quantitative image analysis showed a progressive decline in the percentage of EdU-positive cells with increasing extract concentrations (40, 80, and 160 µg/mL), confirming impaired cell proliferation in a dose-dependent manner (Figures 4B and C).

Western Blotting Analysis

Western blot analysis targeting key hub proteins identified from network pharmacology (STAT3, SRC, and MAPK1) demonstrated a dose-dependent downregulation in their expression levels in MCF-7 cells (Figure 4D). Densitometric quantification confirmed that the extract treatment significantly reduced protein levels relative to the untreated control, aligning with the observed cellular and molecular effects (Figure 4E).

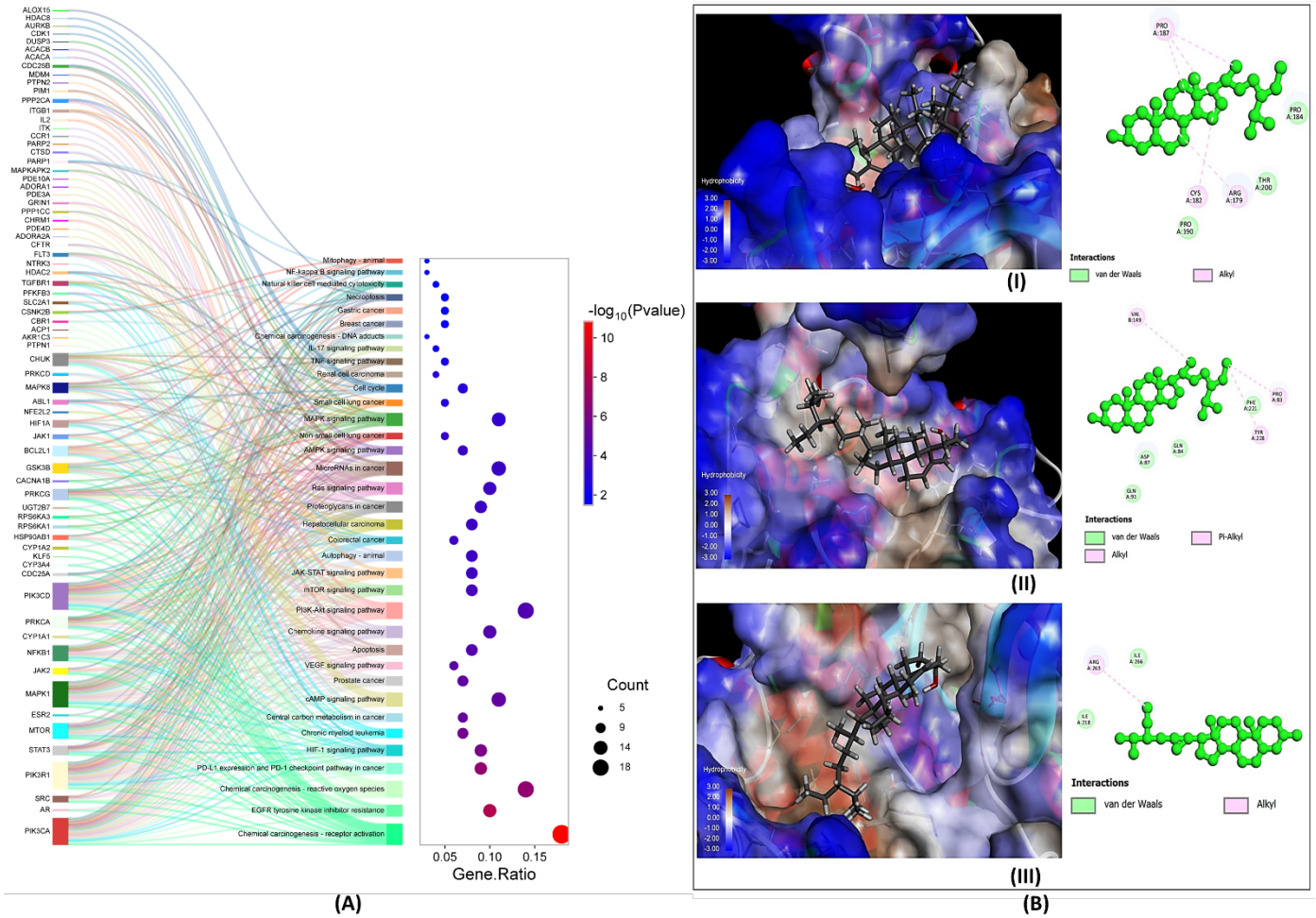

Figure 2: (A) KEGG Pathway Enrichment Analysis: Visualization of enriched KEGG pathways as Sankey plot derived from the common targets, illustrating multiple significant pathways, including chemical carcinogenesis via receptor activation, insulin resistance, EGFR tyrosine kinase inhibitor resistance, and the PD-1/PD-L1 checkpoint pathway, among others. (B) Molecular Docking of Sitogluside with Hub Proteins: Representative docking poses from DockThor showing the binding interactions between sitogluside and key hub proteins (STAT3 (I), SRC (II), and MAPK1 (III)). The figure highlights significant docking scores and specific molecular interactions that support the compound's potential inhibitory effects on these targets.

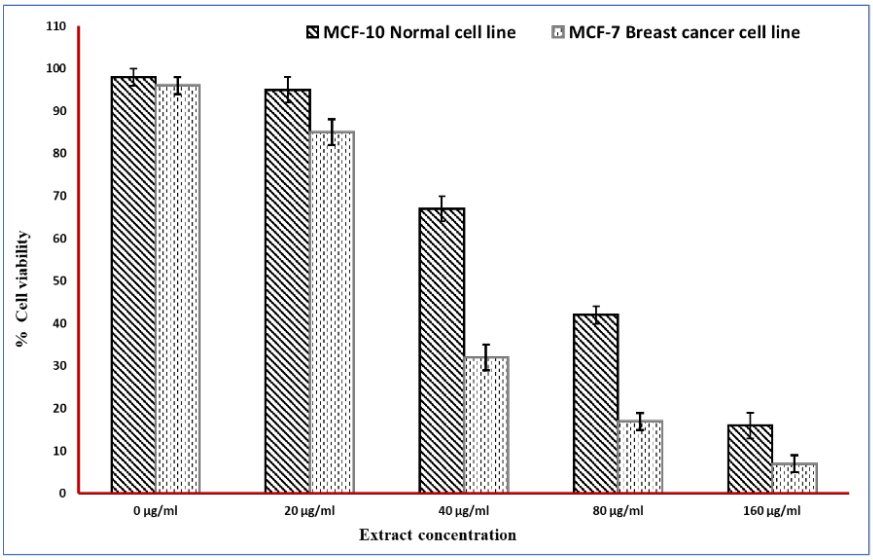

(A)

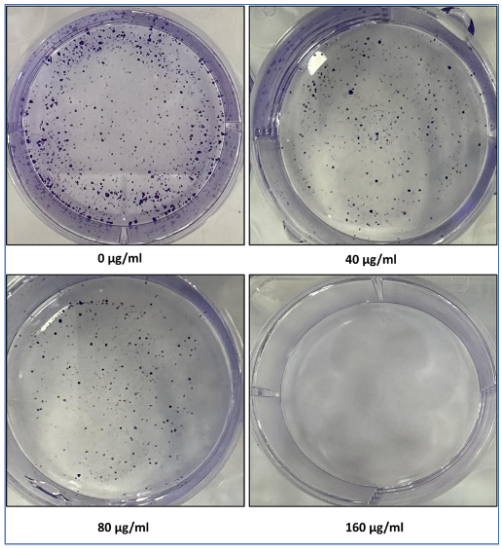

(B)

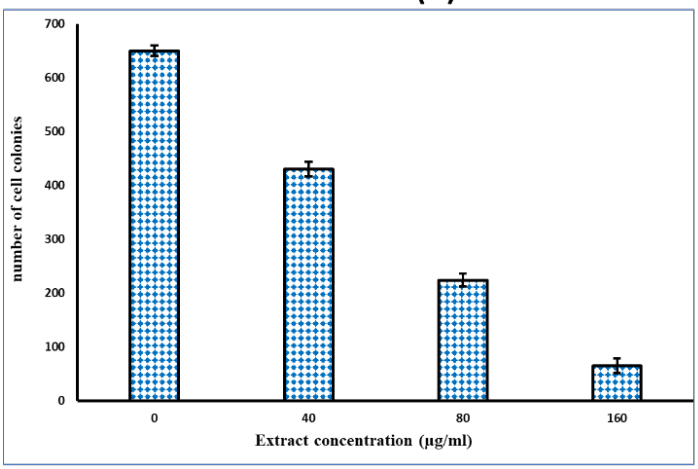

(C)

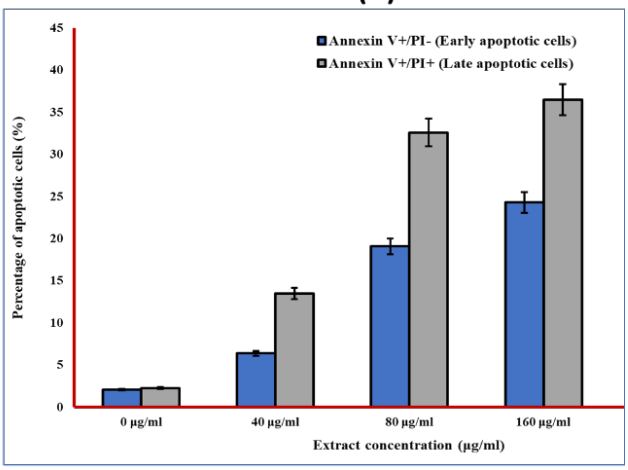

(D)

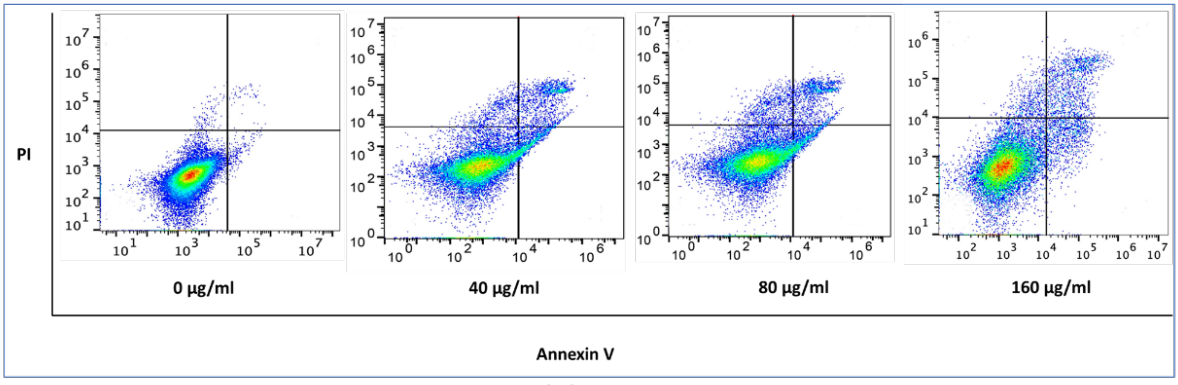

(E)

Figure 3: (A) MTT Cytotoxicity Assay: Bar graph depicting the dose-dependent decrease in cell viability of MCF-7 breast cancer cells following treatment with *Angelica dahurica* extract. Viability is significantly reduced at concentrations of 40, 80, and 160 µg/mL compared to the untreated control, with a more moderate effect observed in MCF-10 cells. (B) Clonogenic Assay - Colony Formation: Representative microscopic images showing a marked reduction in colony formation of MCF-7 cells after 24-hr extract exposure followed by 14 days of growth. Fewer and smaller colonies are evident as the extract concentration increases. (C) Clonogenic Assay - Survival Fraction: Quantitative analysis of clonogenic assay results presented as a survival fraction graph. Data indicate a significant, dose-dependent decline in the clonogenic potential of MCF-7 cells upon extract treatment. (D) Annexin V/PI Apoptosis Analysis: It presents the quantitative analysis of early and late apoptotic cell populations. Both panels demonstrate a significant, dose-dependent increase in apoptosis following extract treatment. (E) It shows representative flow cytometry dot plots of Annexin V/PI-stained MCF-7 cells.

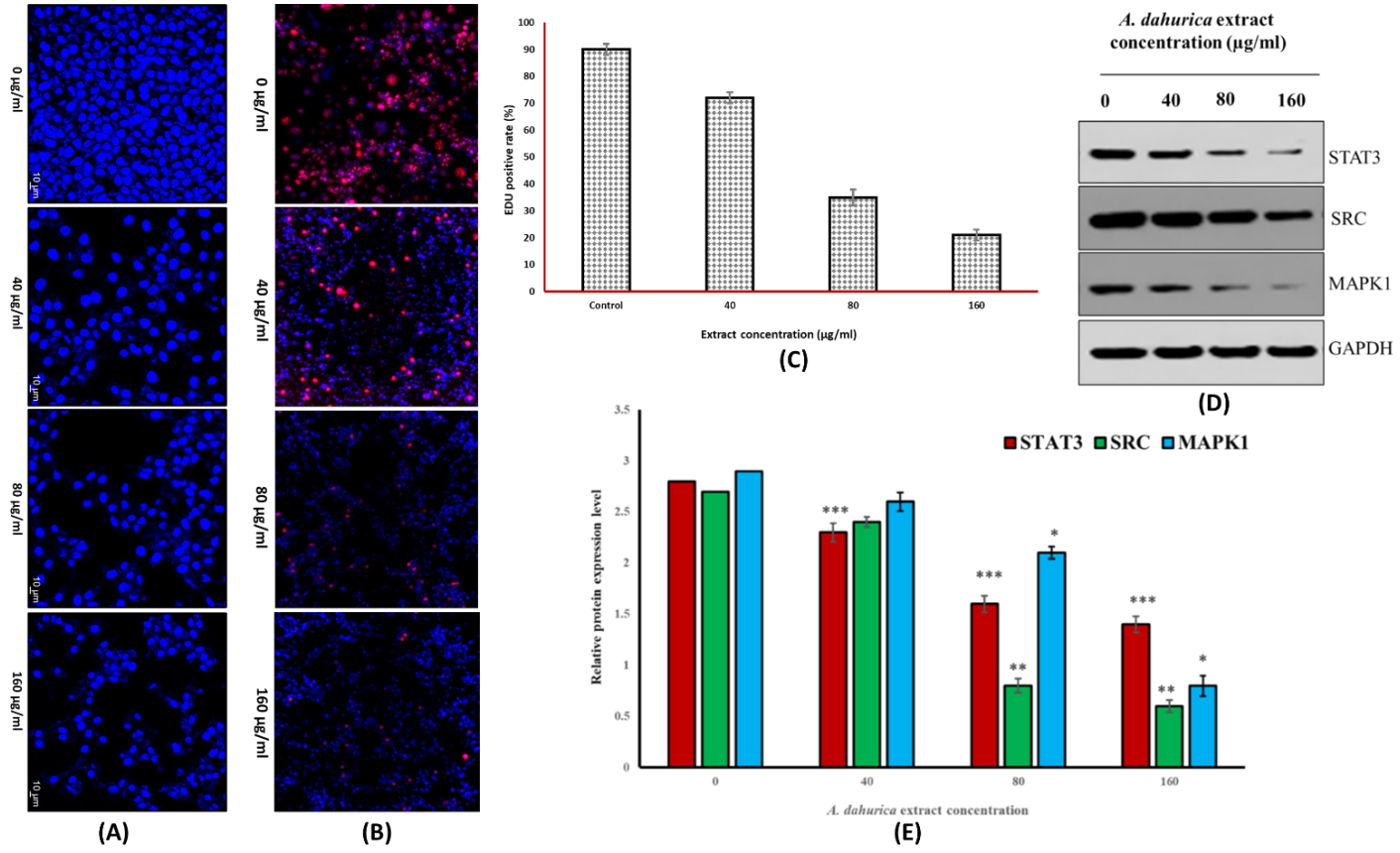

Figure 4: (A) DAPI Staining for Nuclear Morphology: Fluorescence images of DAPI-stained MCF-7 cells illustrating pronounced nuclear alterations (chromatin condensation and fragmentation) at escalating extract concentrations. These nuclear changes are indicative of apoptosis. (B and C) EdU Proliferation Assay: Fluorescence microscopy images and corresponding quantification graph depicting a progressive decrease in EdU-positive MCF-7 cells with increasing extract concentrations, indicating substantial suppression of DNA synthesis and cell proliferation. (D) Western Blot Analysis of Hub Protein Expression: Representative Western blot images showing the expression levels of STAT3, SRC, and MAPK1 in MCF-7 cells treated with varying concentrations of *Angelica dahurica* extract. A clear dose-dependent reduction in band intensities is evident compared to the untreated control. (E) Densitometric Quantification of Western Blots: Bar graph representing the densitometric analysis of STAT3, SRC, and MAPK1 protein bands. The data confirm a statistically significant, dose-dependent downregulation of these hub proteins following extract treatment, corroborating the observed *in vitro* effects.

DISCUSSION

The PPI networks are indispensable in network pharmacology for mapping molecular interactions, identifying key targets, and elucidating multi-target mechanisms, particularly for complex herbal medicines. In our *Angelica dahurica* study, the PPI network was critical in identifying STAT3, SRC, and MAPK1 as hub targets, guiding *in silico* predictions and *in vitro* validation, and highlighting the extract's therapeutic promise in breast cancer treatment by disrupting interconnected oncogenic pathways. These proteins serve as pivotal nodes in signalling cascades that regulate cell proliferation, survival, and apoptosis-pathways essential for breast cancer advancement.

Signal-Transducer and Activator of Transcription-3 (STAT3) is pivotal for oncogenesis.[19] The *in silico* network pharmacology method, which combined target prediction with subsequent PPI analysis, revealed STAT3 as a major hub gene. The docking tests, especially with sitogluside-one of the 13 phytochemicals retrieved from the TCMSP database-demonstrated considerable binding affinity to STAT3, indicating that the molecule may directly interact with and possibly suppress STAT3 activity. The identification aligns with the established function of STAT3 in regulating genes associated with cell survival, proliferation, and inflammation.[20,21] *In vitro*, Western blot analysis demonstrated a dose-dependent reduction of STAT3 in MCF-7 breast cancer cells after treatment with the extract. The decrease in STAT3 expression corresponded with the cell viability reduction, suppression of colony formation, and initiation of apoptosis. Given that STAT3 is often constitutively active in several malignancies, its downregulation is expected to impair essential survival pathways in tumour cells.[22] The reduction of STAT3 activity may result in less transcription of genes that encode anti-apoptotic proteins, thereby making cancer cells more vulnerable to programmed cell death. Furthermore, STAT3 participates in the control of the tumour microenvironment and immune evasion; hence, its suppression may further diminish tumour aggressiveness.

SRC, a non-receptor tyrosine kinase, is a crucial element of carcinogenic signalling networks.[23,24] SRC, recognised as a hub gene in network pharmacology and PPI analysis, has a pivotal role

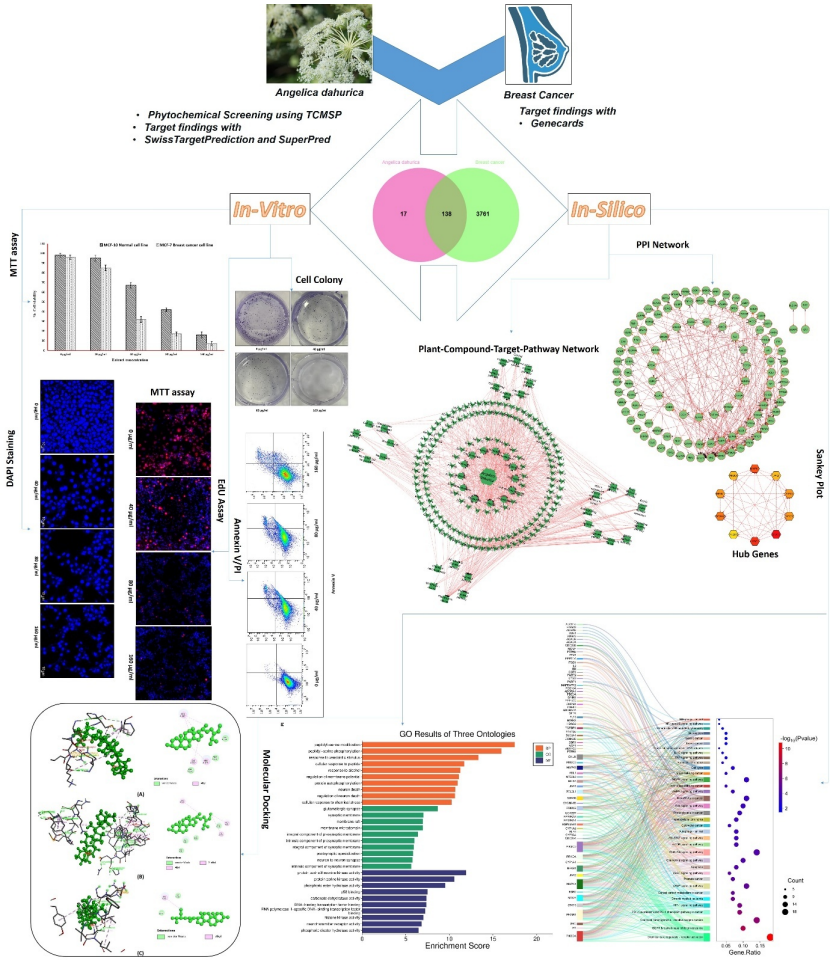

Supplementary Figure 1: Flow Diagram showing study plan and execution sequence.

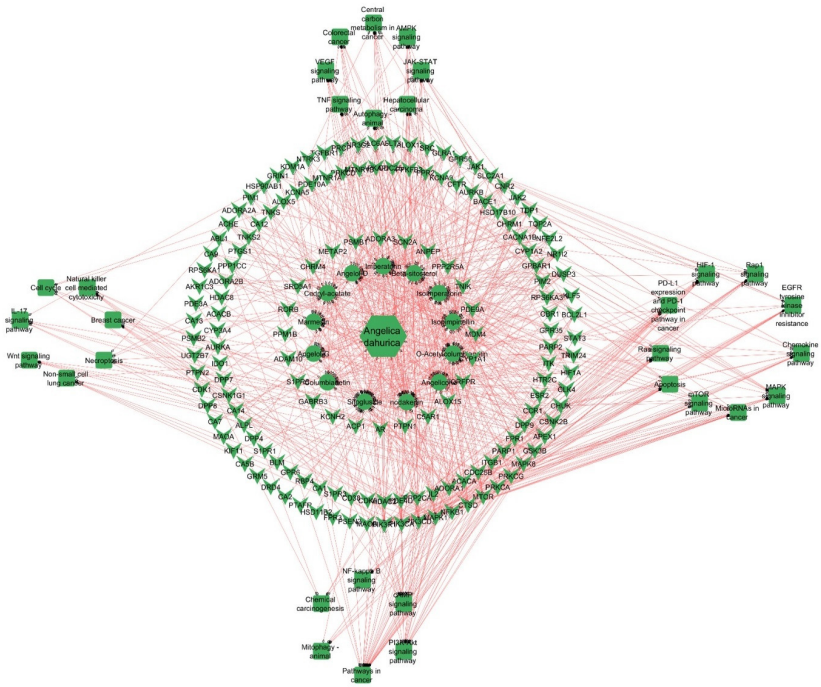

Supplementary Figure 2: Integrated Compound-Target-Pathway Network: Combined network diagram depicting the interactions between plant-derived compounds, identified targets, and enriched signaling pathways. This integrative visualization underscores the multi-target mechanism through which Angelica dahurica compounds may exert anticancer effects.

in controlling cell adhesion, migration, and proliferation, making it a significant target in cancer therapies. Molecular docking experiments revealed that sitogluside had a substantial binding affinity with SRC, indicating that it may inhibit SRC's kinase activity. The *in vitro* experiments corroborate this *in silico* as well. The MTT cytotoxicity experiment revealed that treatment with the *Angelica dahurica* extract significantly decreased cell viability, especially in malignant MCF-7 cells relative to MCF-10 cells. This selective toxicity suggests the capacity of the compound to target abnormal signalling pathways exclusive to cancer cells, possibly those driven by SRC. The clonogenic experiment demonstrated a significant decrease in the capacity of MCF-7 cells to form colonies, partially influenced by SRC-mediated signalling that enhances cell survival and proliferation.[25,26] The extract may inhibit SRC's activity, potentially disrupting downstream signalling pathways that facilitate tumour cell invasion and metastasis, therefore hindering the advancement of breast cancer.

MAPK1, or ERK2, is a pivotal component of the Mitogen-Activated-Protein-Kinase (MAPK) family, essential for the regulation of cell cycle progression, differentiation, and survival.[27,28] The *in silico* assessment retrieved MAPK1 as a pivotal hub protein within the protein-protein interaction network derived from overlapping targets of phytochemicals and breast cancer-associated genes. Docking simulations demonstrated that sitogluside binds proficiently with MAPK1, suggesting its potential to reduce the enzymatic activity of this kinase and, therefore, diminish the proliferative signals in tumour cells. The EdU incorporation test, used to evaluate cellular proliferation, demonstrated a distinct, dose-dependent reduction in DNA synthesis in MCF-7 cells post-treatment with the extract. The decrease in proliferation is directly associated with the disruption of MAPK1-mediated signalling pathways, since MAPK1 plays a crucial role in conveying mitogenic signals from cell surface receptors to the nucleus.[29,30] Furthermore, Western blot analysis revealed a substantial reduction in MAPK1 protein levels in treated cells, indicating that the extract not only disrupts the function but also the production of this essential kinase. The cumulative impact of MAPK1 inhibition likely leads to cell cycle arrest and amplifies the pro-apoptotic response shown in the Annexin V/PI apoptosis experiment.

Network pharmacology is crucial in TCM and anticancer drug discovery, providing a holistic framework to analyze the multi-target actions of herbal compounds. Unlike single-target approaches, it integrates bioinformatics and systems biology to map interactions between compounds, genes, and pathways, identifying active constituents, molecular mechanisms, and synergistic effects. In TCM, it connects traditional knowledge with modern insights, accelerating the discovery of effective, low-toxicity anticancer therapies.

The integration of *in silico* predictions and *in vitro* validations reveals that the anticancer efficacy of *Angelica dahurica* extract is facilitated by a coordinated action on STAT3, SRC, and MAPK1. The *in silico* network analysis delineated these proteins as pivotal to the molecular interactions between bioactive chemicals and breast cancer pathogenesis. Subsequent molecular docking experiments demonstrated the ability of sitogluside to bind efficiently with various targets, offering mechanistic insight into how these interactions may result in functional inhibition. The experimental setting demonstrated evident, dose-dependent cytotoxicity of the extract, which inhibited clonogenic potential, indicating a strong antiproliferative action. The reduced proliferation, shown in the EdU test, together with the notable induction of apoptosis shown in the Annexin V/PI assay, further supports the concept that targeting these signalling hubs impairs critical survival pathways in breast cancer cells. The decrease in STAT3, SRC, and MAPK1 protein levels seen in Western blot analyses correlates with the computational predictions and physiological responses, underscoring the translational significance of these targets. These findings together indicate that *Angelica dahurica* extract, particularly its component sitogluside, may serve as a potential therapeutic agent by influencing several carcinogenic pathways.

CONCLUSION

The integrated *in silico* and *in vitro* findings demonstrate that *Angelica dahurica* extract exerts potent anticancer effects against breast cancer by targeting key oncogenic pathways, including STAT3, SRC, and MAPK1. *In silico* network pharmacology and molecular docking identified these proteins as critical targets, supported by *in vitro* assays showing dose-dependent cytotoxicity, reduced proliferation, suppressed clonogenic potential, and enhanced apoptosis in MCF-7 cells. The downregulation of STAT3, SRC, and MAPK1 highlights a multi-target mechanism disrupting vital survival pathways, emphasizing the extract's therapeutic potential for breast cancer treatment, though further preclinical evaluation is warranted.

ACKNOWLEDGEMENT

None.

ABBREVIATIONS

TCMSP: Traditional Chinese Medicine Systems Pharmacology; **ADME:** Absorption, Distribution, Metabolism, and Excretion; **OB:** Oral Bioavailability; **DL:** DrugLikeness; **PPI:** Protein-Protein Interaction; **GO:** Gene Ontology; KEGG: Kyoto Encyclopedia of Genes and Genomes; **DMEM:** Dulbecco's Modified Eagle's Medium; **FBS:** Fetal Bovine Serum; **MTT:** 3(4,5Dimethyl thiazol2yl)2,5Diphenyl Tetrazolium Bromide assay; **EdU:** 5Ethynyl2′deoxyuridine; **SDSPAGE:** Sodium Dodecyl Sulfate Polyacrylamide Gel Electrophoresis.

CONFLICT OF INTEREST

The authors declare that there is no conflict of interest.

SUMMARY

The phytochemical study of *Angelica dahurica* yielded 99 different compounds, however only 13 of those compounds exhibited desirable properties such as oral bioavailability (≥30%), drug similarity (≥0.18), and Caco 2 permeability. Subsequent target prediction across SwissTargetPrediction and SuperPred yielded 155 unique protein targets. Breast cancer-associated targets from GeneCards (GIFTS score ≥ 55%) numbered 3,899; their intersection with phytochemical targets comprised 138 shared proteins. These showed a protein-protein interaction network of 114 nodes and 293 edges. Network topology assessment highlighted ten hub genes: STAT3, SRC, MAPK1, HSP90AB1, MTOR, HIF1A, NFKB1, JAK2, PIK3CA, and PIK3R1. Functional enrichment revealed key biological processes-peptidylserine phosphorylation, response to xenobiotic stimulus, cellular responses to peptides and alcohol, regulation of membrane potential, protein autophosphorylation, and neuron death regulation. Cellular component terms included glutamatergic synapse, membrane raft, microdomain, and presynaptic membrane; molecular functions centered on protein serine/threonine kinase activity, phosphoric ester hydrolase activity, p53 binding, DNAbinding transcription factor activity, histone kinase activity, and neurotransmitter receptor activity. Pathway analysis implicated chemical carcinogenesis via receptor activation, insulin resistance, EGFRTKI resistance, sphingolipid signalling, pancreatic cancer, neurotrophin signalling, acute myeloid leukemia, ROSmediated carcinogenesis, prolactin signalling, and PDL1/PD1 pathways. Molecular docking identified Sitogluside with docking scores of -9.092 kcal/mol (STAT3), -7.935 (SRC), and -8.400 (MAPK1). *In vitro*, MCF7 viability decreased significantly from 40 µg/mL, with further reductions at 80 and 160 µg/mL; clonogenic survival dropped dosedependently, reaching minimal colonies at 160 µg/mL. EdU assays showed reduced DNA synthesis at 40, 80, and 160 µg/mL. Apoptosis assays revealed increased Annexin V positivity at 80 and 160 µg/mL alongside DAPIdetected nuclear fragmentation. Western blots confirmed dosedependent downregulation of STAT3, SRC, and MAPK1, aligning experimental findings with network predictions.

REFERENCES

1. Adams M. Epidemiology and the leading causes of death. In: Epidemiology for athletic trainers. Routledge; 2024: 3-19. doi: 10.4324/9781003523994-2.
2. Burguin A, Diorio C, Durocher F. Breast cancer treatments: updates and new challenges. J Pers Med. 2021;11(8):808. doi: 10.3390/jpm11080808, PMID 34442452.
3. Liu S, Zhu JJ, Li JC. The interpretation of human body in traditional Chinese medicine and its influence on the characteristics of TCM theory. Anat Rec (Hoboken). 2021;304(11):2559-65. doi: 10.1002/ar.24643, PMID 34117702.
4. Zhao H, Feng YL, Wang M, Wang JJ, Liu T, Yu J. The *Angelica dahurica*: a review of traditional uses, phytochemistry and pharmacology. Front Pharmacol. 2022;13:896637. doi: 10.3389/fphar.2022.896637, PMID 35847034.
5. Wang Q, Li Y, Wang S, Xiang Z, Dong W, Li X, *et al.* A review of the historical records, chemistry, pharmacology, pharmacokinetics and edibility of *Angelica dahurica*. Arab J Chem. 2023;16(8):104877. doi: 10.1016/j.arabjc.2023.104877.
6. Shi H, Chang YQ, Feng X, Yang GY, Zheng YG, Zheng Q, *et al.* Chemical comparison and discrimination of two plant sources of *Angelicae dahuricae* Radix, *Angelica dahurica* and *Angelica dahurica* var. formosana, by HPLC-Q/TOF-MS and quantitative analysis of multiple components by a single marker. Phytochem Anal. 2022;33(5):776-91. doi: 10.1002/pca.3129, PMID 35470493.
7. Zhao L, Zhang H, Li N, Chen J, Xu H, Wang Y, *et al.* Network pharmacology, a promising approach to reveal the pharmacology mechanism of Chinese medicine formula. J Ethnopharmacol. 2023;309:116306. doi: 10.1016/j.jep.2023.116306, PMID 36858276.
8. Zhang P, Zhang D, Zhou W, Wang L, Wang B, Zhang T, *et al.* Network pharmacology: towards the artificial intelligence-based precision traditional Chinese medicine. Brief Bioinform. 2023;25(1):bbad518. doi: 10.1093/bib/bbad518, PMID 38197310.
9. Zheng YM, Shen JZ, Wang Y, Lu AX, Ho WS. Anti-oxidant and anti-cancer activities of *Angelica dahurica* extract via induction of apoptosis in colon cancer cells. Phytomedicine. 2016;23(11):1267-74. doi: 10.1016/j.phymed.2015.11.008, PMID 26776960.
10. Luo KW, Sun JG, Chan JY, Yang L, Wu SH, Fung KP, *et al.* Anticancer effects of imperatorin isolated from *Angelica dahurica*: induction of apoptosis in HepG2 cells through both death-receptor- and mitochondria-mediated pathways. Chemotherapy. 2011;57(6):449-59. doi: 10.1159/000331641, PMID 22189406.
11. Bugnon M, Röhrig UF, Goullieux M, Perez MA, Daina A, Michielin O, *et al.* SwissDock 2024: major enhancements for small-molecule docking with Attracting Cavities and AutoDock Vina. Nucleic Acids Res. 2024; 52(W1):W324-32. doi: 10.1093/nar/gkae300 , PMID 38686803.
12. Stelzer G, Rosen N, Plaschkes I, Zimmerman S, Twik M, Fishilevich S, *et al.* The GeneCards suite: from gene data mining to disease genome sequence analyses. Curr Protoc Bioinformatics. 2016;54(1):1.30.1-1.30.33. doi: 10.1002/cpbi.5, PMID 27322403.
13. Szklarczyk D, Kirsch R, Koutrouli M, Nastou K, Mehryary F, Hachilif R, *et al.* The STRING database in 2023: protein-protein association networks and functional enrichment analyses for any sequenced genome of interest. Nucleic Acids Res. 2023; 51(D1):D638-46. doi: 10.1093/nar/gkac1000, PMID 36370105.
14. Guedes IA, Pereira da Silva MM, Galheigo M, Krempser E, de Magalhães CS, Correa Barbosa HJ, *et al.* DockThor-VS: a free platform for receptor-ligand virtual screening. J Mol Biol. 2024;436(17):168548. doi: 10.1016/j.jmb.2024.168548, PMID 39237203.
15. Mi B, Li Q, Li T, Marshall J, Sai J. A network pharmacology study on analgesic mechanism of Yuanhu-Baizhi herb pair. BMC Complement Med Ther. 2020;20(1):284. doi: 10.1186/s12906-020-03078-0, PMID 32948176.
16. Bai L, Zhou H, Xu R, Zhao Y, Chinnaswamy K, McEachern D, *et al.* A potent and selective small-molecule degrader of STAT3 achieves complete tumor regression *in vivo*. Cancer Cell. 2019;36(5):498-511.e17. doi: 10.1016/j.ccell.2019.10.002, PMID 31715132.
17. Breitenlechner CB, Kairies NA, Honold K, Scheiblich S, Koll H, Greiter E, *et al.* Crystal structures of active SRC kinase domain complexes. J Mol Biol. 2005;353(2):222-31. doi: 10.1016/j.jmb.2005.08.023, PMID 16168436.
18. Park E, Rawson S, Li K, Kim BW, Ficarro SB, Pino GG, *et al.* Architecture of autoinhibited and active BRAF-MEK1-14-3-3 complexes. Nature. 2019;575(7783):545-50. doi: 10.1038/s41586-019-1660-y, PMID 31581174.
19. Hu Y, Dong Z, Liu K. Unraveling the complexity of STAT3 in cancer: molecular understanding and drug discovery. J Exp Clin Cancer Res. 2024;43(1):23. doi: 10.1186/s13046-024-02949-5, PMID 38245798.
20. Dinakar YH, Kumar H, Mudavath SL, Jain R, Ajmeer R, Jain V. Role of STAT3 in the initiation, progression, proliferation and metastasis of breast cancer and strategies to deliver JAK and STAT3 inhibitors. Life Sci. 2022;309:120996. doi: 10.1016/j.lfs.2022.120996, PMID 36170890.
21. Huang B, Lang X, Li X. The role of IL-6/JAK2/STAT3 signaling pathway in cancers. Front Oncol. 2022;12:1023177. doi: 10.3389/fonc.2022.1023177, PMID 36591515.
22. Sadrkhanloo M, Entezari M, Orouei S, Ghollasi M, Fathi N, Rezaei S, *et al.* STAT3-EMT axis in tumors: modulation of cancer metastasis, stemness and therapy response. Pharmacol Res. 2022;182:106311. doi: 10.1016/j.phrs.2022.106311, PMID 35716914.
23. Wang HQ, Man QW, Huo FY, Gao X, Lin H, Li SR, *et al.* STAT3 pathway in cancers: past, present, and future. Med. 2022;3(2):e124. doi: 10.1002/mco2.124, PMID 35356799.
24. Pelaz SG, Tabernero A. Src: coordinating metabolism in cancer. Oncogene. 2022;41(45):4917-28. doi: 10.1038/s41388-022-02487-4, PMID 36217026.
25. Luo J, Zou H, Guo Y, Tong T, Ye L, Zhu C, *et al.* SRC kinase-mediated signaling pathways and targeted therapies in breast cancer. Breast Cancer Res. 2022;24(1):99. doi: 10.1186/s13058-022-01596-y, PMID 36581908.
26. Li L, Deng CX, Chen Q. SRC-3, a steroid receptor coactivator: implication in cancer. Int J Mol Sci. 2021;22(9):4760. doi: 10.3390/ijms22094760, PMID 33946224.
27. Wang Y, Guo Z, Tian Y, Cong L, Zheng Y, Wu Z, *et al.* MAPK1 promotes the metastasis and invasion of gastric cancer as a bidirectional transcription factor. BMC Cancer. 2023;23(1):959. doi: 10.1186/s12885-023-11480-3, PMID 37817112.
28. Lu M, Gao Q, Wang Y, Ren J, Zhang T. LINC00511 promotes cervical cancer progression by regulating the miR-497-5p/MAPK1 axis. Apoptosis. 2022;27(11-12):800-11. doi: 10.1007/s10495-022-01768-3, PMID 36103025.

29. Petrosino M, Novak L, Pasquo A, Turina P, Capriotti E, Minicozzi V, *et al.* The complex impact of cancer-related missense mutations on the stability and on the biophysical and biochemical properties of MAPK1 and MAPK3 somatic variants. Hum Genomics. 2023;17(1):95. doi: 10.1186/s40246-023-00544-x, PMID 37891694.

30. Li M, Cai O, Yu Y, Tan S. Paeonol inhibits the malignancy of Apatinib-resistant gastric cancer cells via LINC00665/miR-665/MAPK1 axis. Phytomedicine. 2022;96:153903. doi: 10.1016/j.phymed.2021.153903, PMID 35026514.

Cite this article: Li Y, Zhao C, Ren Y, Xie L. Anticancer Activity of *Angelica dahurica* Used in Traditional Chinese Medicine (TCM) against Human Breast Cancer Cells: Mechanistic Evaluation by Using an Integrated Approach of Network Pharmacology, Computational Molecular Docking and Experimental Assays. Indian J of Pharmaceutical Education and Research. 2026;60(3):1131-42.

Supplementary Table 1: Bioactive phytochemicals of *Angelica dahurica* retrieved from the TCMSP database which survived screening criteria.

Mol ID	Molecule Name	OB (%)	DL	Structure	Smile
MOL001575	cedryl acetate	53.94	0.17	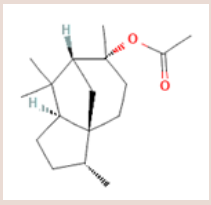	C[C@@H]1CC[C@@H]2[C@]13CC[C@@] ([C@H](C3)C2(C)C) (C)OC(=O)C
MOL001941	imperatorin	34.55	0.22	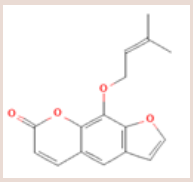	CC(=CCOC1=C2C(=CC3=C1OC=C3)C= CC(=O)O2)C
MOL001942	Isoimperatorin	45.46	0.23	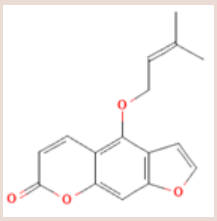	CC(=CCOC1=C2C=CC(=O)OC2=CC3= C1C=CO3)C
MOL001944	Marmesin	50.28	0.18	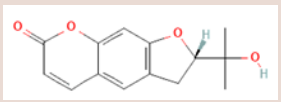	CC(C)([C@@H]1CC2=C(O1)C=C3C (=C2)C=CC(=O)O3)O
MOL003561	Isopimpinellin	25.93	0.17	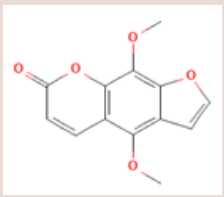	COC1=C2C=COC2=C(C3=C1C=CC (=O)O3)OC
MOL000357	Sitogluside/Daucosterol	20.63	0.62	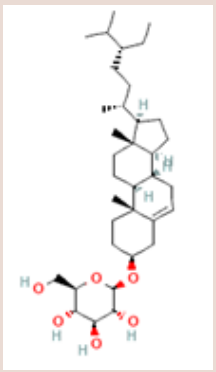	CC[C@H](CC[C@@H](C)[C@H] 1CC[C@@H] 2[C@@]1(CC[C@H]3[C@H]2CC=C4[C@@]3(CC[C@@H] (C4) O[C@H]5[C@@H]([C@H]([C@@H]([C@H](O5)CO)O)O)O)C) C)C(C)C
MOL000358	Beta-sitosterol	36.91	0.75	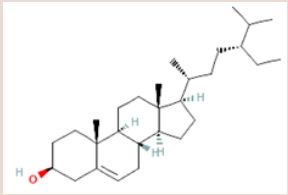	CC[C@H](CC[C@@H](C)[C@H]1CC[C@@H]2 [C@@]1(CC[C@H]3[C@H]2CC=C4[C@@] 3(CC [C@@H](C4)O) C)C)C(C)C

Mol ID	Molecule Name	OB (%)	DL	Structure	Smile
MOL003608	O-Acetylcolumbianetin	60.04	0.26	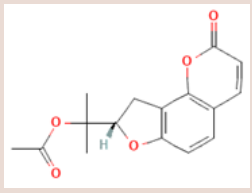	CC(=O)OC(C)(C)[C@@H]1CC2=C(O1)C=CC3=C2OC(=O)C=C3
MOL003609	Columbianetin	32.11	0.17	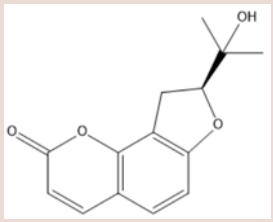	CC(C)([C@@H]1CC2=C(O1) C=CC3=C2OC(=O)C=C3)O
MOL004777	Angelol D	34.85	0.34	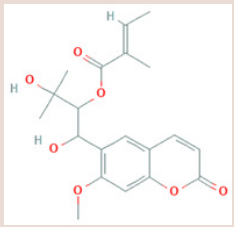	C/C=C(\C)/C(=O)OC(C(C1=C(C=C2C(=C1)C=CC(=O)O2)OC)O)C(C)(C)O
MOL004778	Angelol G	46.03	0.34	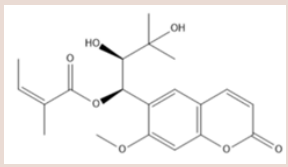	C/C=C(/C)\C(=O)O[C@H](C1=C(C=C2C(=C1)C=CC(=O)O2)OC)[C@H](C(C)(C)O)O
MOL004780	Angelicone	30.99	0.19	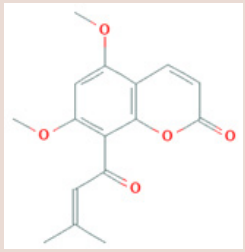	CC(=CC(=O)C1=C(C=C(C2=C1OC(=O)C=C2)OC)OC)C
MOL004792	nodakenin	57.12	0.68	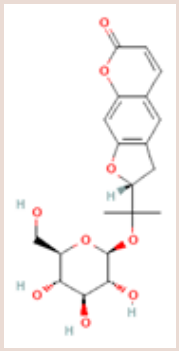	CC(C)([C@H]1CC2=C(O1)C=C3C(=C2)C=CC(=O)O3)O[C@H]4[C@@H]([C@H]([C@@H]([C@H](O4)CO)O)O)O

Supplementary Table 2: Predicted targets of 13 active compounds from *Angelica dahurica* identified using SwissTargetPrediction and SuperPred (≥75% probability).

APEX1	PARP2	UGT2B7	KDM1A	HDAC2	RPS6KA3
CLK4	TNKS2	ACACA	NTRK3	DPP9	ADORA2B
TRIM24	TNKS	ACACB	AR	KCNA5	ADORA3
ALOX12	PDE9A	GPR35	FPR2	CHUK	PRKCG
TDP1	PDE10A	PSMB1	PSMB2	MAOA	PRKCA
TOP2A	GSK3B	MTNR1B	AKR1C3	KCNA3	ABL1
CTSD	MAPK8	SRC	KCNH2	BACE1	PARP1
DUSP3	ADORA2A	TGFBR1	HDAC8	CYP1A2	MAPKAPK2
KLF5	HSD17B10	PIM1	ITK	GABRB3	CSNK1G1
NFE2L2	GLRA1	PIM2	ESR2	SRD5A1	CHRM1
HIF1A	CNR2	CA1	STAT3	CA12	KIF11
SLC2A1	PRCP	ALPL	MTOR	ALOX5	ADAM10
SLC6A5	HTR2C	AURKB	PRKCD	MAOB	CHRM4
NR1I2	CCR1	AURKA	BLM	ALOX15	IL2
NFKB1	MDM4	JAK1	CDK1	CD38	BCL2L1
DPP8	FPR1	JAK2	IDO1	CA7	PSEN2
CSNK2B	C5AR1	PIK3CA	CYP3A4	CA14	PTAFR
PDE3A	DPP4	RPS6KA1	S1PR5	CA13	S1PR3
GPR55	DPP7	TNIK	HSP90AB1	CA5B	S1PR1
RORB	CACNA1B	QRFPR	PIK3R1	CBR1	PTPN2
METAP2	GPBAR1	PPP2R5A	SCN2A	PIK3CD	CDC25B
PDE4D	ADORA1	HSD11B2	FPR3	MAPK1	ACP1
CA9	PTGS1	DRD4	ACHE	ANPEP	PPM1B
FLT3	NR3C2	RBP4	PTPN1	CYP1A1	PPP1CC
MTNR1A	GRIN1	PFKFB3	CDC25A	CA2	PPP2CA
CFTR	ITGB1	GPR6	GRM5	CDK5	

Supplementary Table 3: Breast cancer–related targets retrieved from GeneCards database filtered by GIFTS score ≥55%.

BRCA2	AURKB	AMACR	IRF8	CUL2	PGM3	UGT8	SLC26A3
BRCA1	EPAS1	AZGP1	RPS27	ARHGDIB	SFTPD	MCOLN1	CHRNA1
ATM	APOB	CTSL	ICOS	TNFRSF17	ATXN2	GABARAPL2	FGG
PALB2	HSPA5	EED	STRADA	BMX	SGPL1	TDO2	NDUFA12
BRIP1	TLR2	KLK2	CTBP2	BANF1	LAMA4	CAMK4	SGCE
CHEK2	PLCG1	CASP2	ACVR2A	PLD1	ATP5F1B	TBC1D4	TUB
BARD1	LGALS3	EIF2AK2	RAD17	NID1	PHF8	CHRNA2	EARS2
CDH1	HSPA4	PLG	CDK9	BMP1	GNAI2	MICU1	MINK1
TP53	NRP1	CDH11	GLUL	IL12A	OAS1	GGCX	ACACB
MSH6	GNRHR	MAP2K3	TYRP1	UGT1A6	PIBF1	NPEPPS	NDST1
MSH2	SGK1	DVL1	PRKAB1	FOXO4	ADH1A	F8	SLC9A3
MLH1	EPHA3	MYH7	F2	GLUD1	LIPE	PCYT1A	HIBCH
APC	FGF4	F2RL1	PPP5C	MB	NOP56	ACADM	PHEX
PMS2	DDR2	XPO1	RPL15	ALOX15	GLRX	PYGB	APBB1
PTEN	PROM1	MAPK7	FLI1	MFN2	CACNA1H	GJB6	SLC25A12
EGFR	TMPRSS2	PGF	EPHA7	GFRA1	PDX1	ACSL1	GRHPR
RAD50	TRRAP	POLH	ALDH9A1	PTPRO	DGKE	HCN1	AMPD2
NF1	SHBG	COPS5	ADM	IRF6	C5	NSF	PLA2G1B
RAD51C	IRS2	IL1R1	SPTAN1	CD38	CSPG4	APOL1	CALB1
ERBB2	CD36	CEACAM1	SIRT6	CTPS1	PTX3	LIPC	TNR
NBN	RUNX3	VCL	DNM2	PSEN1	F13A1	PSMB7	DRD5
POLD1	ADIPOQ	OTC	RAN	ANGPTL4	SOX6	DCT	CRB1
POLE	KCNH2	SOS2	MDK	SCD	UBE2L3	IL10RB	RDH12
STK11	ARAF	NAMPT	STAT4	KIF2C	GALNS	GDF5	SCN1B
AXIN2	NOS3	GLA	SCN11A	SOX17	RFC2	ATP5PO	CSNK1G1
ESR1	FGF8	FGF19	RPS24	ECE1	POLR3A	PEX5	CHRNA4
PIK3CA	CYP3A4	GHR	FCGR1A	IFNAR1	DHX16	FAM20C	CACNB2
CDKN2A	FOXP3	CSNK2A2	CD151	CDK10	STT3A	CORO1A	UQCRB
MUTYH	KIF1B	LATS2	SNCA	EIF4A2	PSMB4	KLKB1	GYPA
KRAS	HLA-A	CHKA	SOCS2	MAFB	MAPK8IP1	MC4R	HAVCR1
MET	LIG4	CD40LG	MBL2	SORT1	CS	CAMK2B	MTTP
AKT1	TNFRSF8	MCM2	LGMN	MRAS	SLC25A5	GRM6	SARM1
BLM	IL1A	TACSTD2	SMARCC2	ANTXR1	ITPR2	DTNBP1	PISD
RET	XRCC6	ADAM15	IGF2BP2	PLAGL1	GNAI3	ACO1	ABCG5
RB1	JAK3	ELK1	SERPINF1	PPP1CA	YWHAH	TNIK	HAAO
DICER1	UGT1A1	ACP3	SMAD6	FBP1	TECR	GNAO1	INVS
SMAD4	CDC42	UBE2T	PODXL	EGR2	RNASET2	SLC19A2	NDUFB8
TSC2	BCL10	GRPR	RAG1	NEDD4L	EOMES	PNPLA2	GRIA1
MRE11	MMP11	NUMB	BRD3	FTH1	UBB	MYO1E	HAL
SMARCA4	SULT1A1	LRP1	RSPO1	CACNA1G	PSMA4	PPP4C	MSTN
BAP1	PAK4	PPARGC1A	FOXA2	TFAP2B	PLCB2	CNTN6	CHIT1
PTCH1	HMGB1	AKAP13	TAF15	S1PR1	SH2D1A	MASP1	ADAMTS2
KIT	CDC25C	AGTR1	CALCR	CCR3	CHRNA7	SLC8A1	SCN1A

BRCA2	AURKB	AMACR	IRF8	CUL2	PGM3	UGT8	SLC26A3
BRAF	GNAQ	FOSL2	CFL1	ADCYAP1	YWHAG	IDE	HRG
MSH3	ING1	RARG	GATA6	SETD7	ATP6V1B2	B4GALNT1	CES1
EPCAM	CYP2A6	KISS1R	SELL	KIF23	ATP2B1	VAMP1	MOCS2
FANCC	HDAC9	PIK3C3	PDE11A	TLR8	GRIP1	CDC34	GAP43
ALK	BCL2L11	EDN1	UBE3A	SOX3	KRT16	PEX1	KCNA1
BMPR1A	BRD4	CCNH	FSHR	EGLN2	ATN1	PIKFYVE	FARS2
TSC1	KDM1A	HLA-C	PYCR1	TBX2	PPP1R12A	NFATC4	GUCY1A1
CDK4	ROBO1	DMD	MAD2L2	DYRK1B	DNASE1L3	NLGN4X	PLTP
CTNNB1	FGF10	CDH17	PLA2G10	CYSLTR2	LTBP3	BAMBI	CRLF1
AR	NR3C1	DDX3X	PLK3	ARHGEF12	CAMK2D	GOT1	NDUFS7
CCND1	EZR	NFATC1	POLR2A	SOAT1	CTSH	CYC1	PPM1A
MEN1	KRT14	CASP1	PDIA3	KIF5B	NAGLU	GALK1	CLPP
CTNNA1	BMP2	FBLN1	NFIX	DOCK8	ARHGEF7	LGI1	COQ6
SDHA	CHD1	HSD3B2	UGT1A9	NISCH	NR2E3	ALDH1B1	P2RY6
FGFR2	ALDH2	EPO	ATG7	IL18R1	TJP2	LBP	PIGK
FH	BECN1	SLC7A11	NOD2	CNR1	RHOH	ATP1A3	ABCC9
TERT	HLA-B	HSPD1	KCNB2	THBD	PAK2	PKN2	SLC39A14
MYC	PAX8	PTPA	HYAL2	ADCY10	OSMR	HJV	WARS2
SDHB	CFLAR	SREBF1	ITGB6	MEF2C	FRK	PTPRB	APCS
ATR	PRSS1	WNT2	BRD2	S1PR3	CYP26A1	SMS	LSS
RAD51	BCL6	RPS27A	COX5A	PTRH2	SLC46A1	KCNJ3	LINGO1
PDGFRA	CALR	ARID1B	ARRB1	HNMT	RAB23	CHMP2B	PDE3B
HRAS	CTTN	MAPK12	HDAC7	STAG3	SEC31A	ADORA1	KCNB1
FLCN	FGF1	ATP2B4	PC	HMGB2	ADCY5	STAMBP	EBP
NTHL1	TNFSF11	MFGE8	RBPJ	STEAP3	TTPA	SLC38A1	TNNI2
CDKN1B	CTNND1	ASXL1	TNK2	PLXNA1	HCK	COL11A2	NEFM
FANCM	NFKB2	KAT2B	TNFRSF14	S100A10	PLCD1	PLA2G7	ATP6V0A4
FGFR3	CA9	HK1	UNG	CRH	DYNC1H1	DHPS	MOCS1
SDHC	CCL5	USP7	TBK1	FUCA1	P4HA2	PEX19	APOA4
VHL	GJA1	HIP1	PFKFB3	TLE1	KARS1	KYNU	UNC119
MDM2	ERG	CSNK2B	KDM4C	CALM3	CTSF	FPR2	CASQ2
CDC73	DKC1	PTGS1	FUT2	SLC25A13	CDK13	RORC	NR2E1
SDHD	CUL1	ENPP2	RXRB	GOT2	SELPLG	BCS1L	VIPR2
FANCD2	CD28	CCNB2	NTF3	MAK	GCLM	SLC33A1	ROBO4
NRAS	CYP11B1	PON1	PPP1CB	SMARCC1	HTT	FDFT1	GAD2
CASP8	SF3B1	EIF4G3	ACSL4	GDF2	HRH4	HAGH	GRK1
FGFR1	TUBB3	TUBA1B	SMARCAL1	TUBB2A	ABCA2	PCSK2	SLC4A4
RAD54L	MAD1L1	LOXL2	SELENBP1	CYBB	SLCO1B1	LARS1	HTR1B
NF2	CBS	PTH	INHA	SLC31A1	VAPA	PNMT	HTR4
ERCC2	RYR1	ATF4	PLA2G4A	PRDX3	POFUT1	PI4KA	MGAM
RUNX1	GSN	GATA4	WNT2B	ACKR1	MARK2	SLC25A19	PRKAB2
SRC	ANXA2	ALOX5	GNA13	GGH	HSD11B1	SPTLC2	SNAP25
ERBB3	XRCC5	TRAF2	CPA1	PGD	MAP4K2	MMACHC	ECHS1

BRCA2	AURKB	AMACR	IRF8	CUL2	PGM3	UGT8	SLC26A3
PPM1D	MYCN	KRT17	SREBF2	PAX9	MAP2	ADRA1A	ACSS2
TGFBR2	GADD45A	ARHGEF2	FABP3	SET	RAP1B	FGB	NPY5R
ARID1A	IL3	MT2A	KAT2A	FIG4	RPL21	MEF2A	GYPC
CHEK1	SPARC	PFKP	TEAD1	TNKS2	CPE	POMT1	CHRM2
GREM1	FGF7	NR1I2	ANXA3	UCP2	MVK	SERPINA5	KCNQ3
FANCA	BID	FZD7	LEFTY2	SHMT2	MTMR2	TLL1	OSGEP
XRCC3	GDF15	PIAS1	ITGA9	SFTPB	TOLLIP	ALOX5AP	ISCU
EP300	TFAP2A	CDC6	ITGAX	TUBA1A	HARS2	ATP6AP2	ATP1A2
ERBB4	S100A4	CALCA	PAICS	SLCO2A1	TWNK	ISL1	IDUA
POT1	DKK1	SLC3A2	CSNK1E	HTRA2	LMX1B	SEMA7A	TRPM6
PIK3R1	MMP3	BMPR2	BAG3	CYB5R3	CDK19	NARS1	BCKDK
CDK12	ITGA6	IL4R	DES	UBTF	ADGRG1	KCNJ5	ALDH6A1
JUN	KLF5	ISG15	HSD17B4	TNXB	NECTIN1	ETFB	FBP2
CDKN2B	CYP1A2	PIK3R3	CD81	CFL2	CERS2	PSMD7	SLC20A2
CCNE1	TNFRSF10A	DLL4	FST	NUP107	RRM2B	HINT1	CHRND
ABCC1	EIF2B5	HPRT1	FCGR3B	EPHX2	FZD2	NDN	TRAF3IP2
STAT3	TET2	THBS2	CHRNA3	ACY1	EPB41	FDXR	CRYM
LZTR1	IGFBP2	NFATC2	SAT1	CBR1	ACOX1	LIPA	SLC1A7
SMARCB1	NAT1	KCNN3	PPBP	UBE2K	CD96	DIAPH3	CACNA1F
GATA3	RAD21	SP3	FOXC2	MERTK	UBE2D3	GRID2	LY96
PRKAR1A	EXO1	PROX1	RETN	IGFALS	SAG	SCN9A	AKR1D1
CYP17A1	FAP	ADRB2	CGA	AMBP	EIF2B1	TLK2	DPYS
FBXW7	BAD	YWHAE	RAC2	TAPBP	TUBA4A	CACNA1A	DTNA
MAP2K1	TFRC	FYN	FABP7	IRF7	CCT5	EHHADH	ARNT2
WT1	ENO1	FPR1	OXTR	TRIM32	CHRM1	PTDSS1	STX1A
NTRK1	TEK	RICTOR	CDC37	SLC22A3	USP2	BCKDHA	SUOX
BUB1B	PRKCD	FOLR1	GHRHR	NPY	PCCB	CCS	DLG2
CYP19A1	CTSB	EIF4G1	HIPK2	BMP3	RAB7A	COL6A2	SPTA1
HMMR	BSG	SLC9A1	TNFSF4	NOD1	ABCA4	SLC26A2	PDE10A
CDK2	CEBPB	MELK	PAPPA	CASP5	ERLIN2	GRIK1	P2RY12
MAP3K1	CRP	TXNRD1	EPHA4	OCLN	CHST3	MAG	FGFRL1
SUFU	NR1H2	BTC	ENTPD1	SLC28A1	SP7	ESD	MBTPS1
BCL2	GAPDH	CYP11A1	TYRO3	SUMO1	C1S	MAOB	TACR2
PGR	SOCS3	MTAP	EHMT1	AP3B1	ITPKC	IL12RB2	PDE9A
IL2	IL17A	FGF5	SSTR5	DLG1	HRH1	C4BPA	MOG
EZH2	HNRNPK	THY1	TFEB	STING1	CD1D	PSMB10	C2
NOTCH1	PDK1	TBL1XR1	THRB	FAAH	UROD	ADCY1	PTGDR2
KRT19	MPO	EIF4A1	S100B	PTGIS	ATP6V0A2	CTSG	AQP9
CDKN1A	PPARA	PTPRG	CARD11	TRADD	F10	ATP6V1A	MYH6
FANCG	RXRA	CXCR1	HEY1	OGT	ATXN10	GCDH	PRPH
FOXA1	MBD4	PTPRK	FMR1	TCP1	IARS1	NUP155	CHRNG
VEGFA	WNT1	HDAC5	RPS10	GIPC1	ARHGAP1	ARHGEF6	ITGA8
NTRK3	SBDS	CACNA1S	BRCC3	HEXB	STK3	BEST1	KCND2

BRCA2	AURKB	AMACR	IRF8	CUL2	PGM3	UGT8	SLC26A3
HIF1A	FADD	GAB1	HNRNPC	SELP	HSPA1L	FCN2	GJA4
KMT2D	YY1	CHD7	LBR	TPMT	SLIT3	BDH1	TREH
SHC1	TNFRSF1B	PRKCB	PLCE1	PGAM1	CCL7	PTPN22	FYB1
ERCC5	HDAC6	ECM1	CCL11	PITX2	CDC42BPB	SLC20A1	GDA
FANCL	STAT6	RPS6	KRT1	NOX1	GPT2	VLDLR	F9
SMAD7	CD34	PRMT7	RPLP0	ANK1	ATG16L1	SLC52A3	SNTA1
PRKDC	BMP7	VCP	PRKACG	ST3GAL3	FKBP8	PCK2	SLC12A3
WRN	SLC34A2	CD163	HYAL1	PTPN14	LETM1	VKORC1	MCFD2
ERCC4	ITGB3	RPS6KB2	CLIC1	PLEC	STK36	NDUFA8	PDE6C
ITGB1	E2F3	UBC	AMFR	PCSK1	WFS1	TUBA8	CHAT
IL1B	ANXA1	RALA	ACLY	CD226	ADAMTS13	WASF1	ADH4
NTRK2	IL2RA	MYBL2	KPNA2	TDG	PKLR	GALNT2	CPT1B
TGFB1	CASP7	GAS6	ROR1	FGA	RIPK2	AMT	AVPR1A
SMO	EGR1	CD70	ERCC8	SYN1	LDHB	POMGNT1	MANBA
CREBBP	EIF4E	PRKCE	LPAR3	CYBA	LTK	MLKL	COX6A1
MUC1	CCN2	POMC	VDAC1	DDIT4	RAMP2	PSMB1	CACNA1E
HNF1A	KDM5B	EPHA5	SPRY2	HADHB	PINK1	PREP	ST3GAL5
RB1CC1	PDCD1LG2	HSPG2	RNF216	POLR1C	CES2	CLCN1	DAO
DLC1	DSC2	SATB1	GDNF	PFAS	HPD	CNTNAP1	EIF2AK1
AIP	PLK2	STUB1	MDH2	ATP12A	AK2	DAB1	NPR3
PHB1	NDRG1	PTH1R	DRD2	PPP1R3A	PMP22	PDE1C	TRPV3
MSR1	SOX4	PBX1	NTN1	CFH	DPYSL2	BCKDHB	AMPD1
BAX	BCR	NR3C2	NCSTN	ATP5F1A	FOXG1	ARSB	PDE6D
PPARG	FOLH1	TCF4	TTR	PFKL	OAT	APRT	PEX7
MTOR	SYK	NRIP1	FHL2	TUBB6	EPS15	GRB14	CHRNB1
XPC	ITGAV	DPP4	COL5A1	GPHN	MAP4K4	IL1RAP	GFRA2
NCOR1	ADAR	BIN1	RALBP1	KPNB1	MYOF	OPHN1	SCNN1G
AURKA	HMGA1	F5	ABL2	MLXIPL	SLC25A1	CD3E	SLC12A1
MITF	HBEGF	GRM8	DVL3	GRK2	MMADHC	JAM3	CPA6
ATRX	NCOA1	MMP8	RORA	CDC7	MCCC2	TDP2	KCNJ12
CD274	ABCC2	IRF4	NONO	COL4A6	AFG3L2	CRHR2	C9
BCAR1	GNA11	DAB2	ANG	AKR1C4	LIMK2	TRPM1	HCCS
PHOX2B	CHUK	ARG1	CRABP1	POLE2	NR1H3	DMPK	SGSH
MAX	HDAC2	AGER	KAT6A	GNB2	CRHR1	SLC6A6	CAPN5
NRG1	VEGFB	MAP2K5	GPNMB	PCSK7	HEXA	MPI	GABRD
IGF1R	EPOR	LIMK1	DHX9	MAPRE1	ENPEP	KCNJ1	HTR7
TSG101	CCR7	AKR1C2	MAP3K20	LYZ	CTSV	IMPA1	GRM7
MAP2K4	THBS4	ELANE	ATP1A1	YWHAB	EXOSC3	ATP6V1E1	CC2D1A
HFE	CTNNA2	TOP2B	NLRP3	COL6A3	BCHE	HMGCS1	SCN8A
ERCC3	JAG1	SRSF2	TSPO	SLC2A2	PDP1	IDH3B	ANGPTL3
WEE1	FSCN1	SLC29A1	TGFBI	SNRNP200	ALDH7A1	MAN1A2	PLP1
SMAD3	ALB	EIF2S1	LAMC1	CENPE	NR1I3	CDKL5	MTMR14
KDM6A	PCSK9	ESRRB	CRKL	AKR1B1	FLII	DISC1	ETHE1

BRCA2	AURKB	AMACR	IRF8	CUL2	PGM3	UGT8	SLC26A3
ESR2	LGALS1	S100A9	CALD1	SLC17A5	TUBB4B	LTBP2	SCN4B
TGFBR1	PPARD	CENPF	PSMB9	COL4A5	GLP1R	GRIK2	CHRNB2
MAPK1	POSTN	AKR1C1	CYP2C8	TAB2	PI4KB	CAPNS1	PPP3CB
DHFR	IDO1	DDX41	TLR3	RNASE1	GAD1	SLIT1	SLC18A2
IL6	LAMA5	RSPO2	TCF12	RIPK4	KCNK9	ELOVL4	CAV3
FAS	ITGA3	WNT7B	HDAC8	SPTLC1	CITED2	NDUFA10	NPHP1
IGF1	IL18	LPAR1	CILK1	RIGI	CFP	SLC5A6	C1QC
EGF	SOD1	H3-3A	MADD	HGS	BHMT	SLC12A2	DNM1
TP53BP1	CHGA	FCGR3A	CIITA	HNRNPDL	CNP	CKM	IDS
ABCB1	CAT	ACP1	NTSR1	RAC3	ATXN3	PAFAH1B1	DEGS1
IDH1	ANXA5	RAP1A	UBE2N	COL6A1	ATP2A3	IMPDH1	TPK1
IL1RN	BIRC2	ADAM9	RPL18	AARS1	ADARB1	ADCY2	CORIN
KMT2C	SQSTM1	HPGD	EFEMP1	ATP6AP1	PPIB	GAK	F12
EXT2	RACK1	NR5A2	CHD2	ADGRE5	GABBR1	CELF2	HTR1D
PBRM1	MMP13	ALDOA	IRF3	ST3GAL4	ETFA	SARS1	CERS1
RAF1	CD40	TYK2	ASCL1	TRPC6	BCAT1	ABCD3	AASS
IGF2	BDNF	HSD3B1	AICDA	KRT6A	SCNN1A	GRK6	AVPR1B
TP63	JUP	SMC3	KCNA3	SERPINC1	ALAD	CYP26B1	GRIK5
CXCR4	CLU	DAXX	CA2	UGDH	STK39	PPID	QDPR
ABCG2	GLI2	MMP10	UBA1	TCN2	FABP1	RTN4R	SNCB
PTGS2	BAG1	EFNA1	PSMC4	DNM1L	NCK1	TPP2	GRIK4
TNF	ESRRA	PEBP1	RPS6KA3	ACHE	PTPRS	DRD4	PCK1
PIK3CG	PXN	LTF	TAP2	MUSK	YME1L1	GP6	GABRA4
NQO2	REV3L	ACE	BCL11B	HBB	SCNN1B	ETFDH	POMT2
IL7R	CPS1	REL	MAPKAPK2	PURA	PSMD4	NMNAT1	NDUFA9
KDR	RUNX2	ANPEP	TPI1	SFTPA1	HTR2A	RIMS1	ADCYAP1R1
GPC3	LOX	PLCG2	NR2F2	AVPR2	NRG3	GMPS	NOX3
GSTM1	EIF4EBP1	SIX1	LPP	ARCN1	PRICKLE1	SLC34A1	RLBP1
GATA2	IGFBP1	CYP2B6	SMURF1	GRIN2A	ACVR2B	OGDH	AQP4
CDKN1C	NOTCH4	SULT1E1	SALL4	OPRM1	MSRA	SLC10A1	C8B
MKI67	PAX5	PRDX2	HAND2	UGT1A4	LTA4H	IDH3A	SYT2
JAK2	TNFRSF1A	HLA-DQA1	CAV2	TUFM	RIPK3	LRPAP1	LAT
CDK6	TNFRSF11B	HNRNPA2B1	WDR5	TNFSF13	SCN4A	CD3G	ROM1
XPA	NCOA2	EPHX1	GNB1	GPC4	EEA1	NEFL	NAAA
FASLG	LCN2	NR5A1	EPHB6	CNBP	LAMB2	PTPRM	SEC24D
XRCC1	STMN1	ADIPOR1	KIF11	APPL1	LRP2	SALL1	LOXL3
PRKN	RRM1	ROCK2	FGR	COX4I1	CD244	ALDH5A1	HCRTR2
MMP2	PIN1	RPS6KA1	TNFRSF13B	DPF2	RXFP2	CDK16	ACADS
KMT2A	ENO2	ATP6V0A1	AIMP2	DHCR24	OPA1	CASP14	CACNB1
CD44	IGFBP5	IFNA2	IL1R2	ALOX12B	PHKB	PHKA2	MTO1
IDH2	MST1R	CP	MGP	ELP1	BLMH	C1QA	NPC2
PTPN11	PTPRC	KAT5	POLG	CYP27A1	AARS2	NDUFS3	SCN3A
PARP1	VRK1	CRK	ITGA1	MC2R	NPPA	PCBD1	KCNQ2

BRCA2	AURKB	AMACR	IRF8	CUL2	PGM3	UGT8	SLC26A3
FLT1	CUX1	MCM7	ATP7A	MAP1B	TNFRSF25	SLC25A4	KCNJ2
MTHFR	ETV1	BCOR	PBK	PSPH	PTGDR	PDK3	GYS1
NEK2	PDPK1	NRCAM	NHP2	SLC5A1	DLD	TUBB1	JPH2
MMP9	TG	CASP6	MAP2K6	SIK1	HBA1	UNC13B	TRHR
ABCA1	ACACA	PPP2CA	HNRNPU	AQP5	ADSL	LPAR6	PHOX2A
GSTP1	F3	HNRNPA1	SMAD9	PDE5A	MARK3	MPZ	SLC6A8
RASSF1	PHGDH	PTPRF	HLA-DPB1	TBXAS1	ABCB6	LOXL1	GRM5
PTCH2	DUSP6	WIF1	UBE2D1	TLR6	PPP1CC	CALU	KCNK3
SOD2	IGFBP6	MAP3K5	COL7A1	HCFC1	ACAD9	SLC1A2	LIAS
NFE2L2	GPC6	SLC2A3	FDPS	PIK3C2A	PEX14	NFS1	HPCA
NFKB1	HMOX1	HSPA1A	FZD5	NEU1	ATP2B3	TNNT3	XYLT1
SMARCE1	PDCD4	ABI1	DDB1	CTNND2	GNAI1	AP2M1	SLC2A9
BIRC5	CXCL1	CRABP2	KDM2B	ASS1	MMP19	NDUFS2	SLC3A1
LMNA	LATS1	NR0B1	RANBP1	IL10RA	UBR1	PTPN7	KCNA2
RNASEL	IKBKB	PER2	HMBS	BRDT	AVP	SLC27A4	CLN3
DDB2	GSTM3	EEF2	GPC1	TNFSF15	DUT	DRD3	CDH8
SPOP	FEN1	FKBP4	CHD3	PLOD1	AGRN	ANTXR2	CNGA3
CASP3	HPSE	WNT7A	PAX6	DST	RAB5A	COL4A4	GPLD1
NCOA3	RHOB	PSMB8	RPL10	IFNAR2	MAT1A	PEX2	SCN7A
KLC1	IKBKE	FGF18	PRDM16	TXNRD2	LAP3	PON2	VNN1
YAP1	CYP24A1	FURIN	MST1	PLCB1	STIP1	KHK	KCNH5
TFF1	CDK7	FLNA	PRKD3	TUBB2B	PCCA	SLC25A10	TMPRSS15
GNAS	RYR2	RPTOR	PLK4	ADH5	CCR8	PSMB6	MYL1
MGMT	TGIF1	MMP12	UGT2B7	SMYD2	HDAC10	APLP2	GLRA1
ACVR1B	H2AX	AMH	LPL	ABCB7	MYH10	ROBO2	PDE6A
GLI1	HK2	CHD8	LTBP1	CEL	TRPM4	KCNAB2	PCDH19
TYMS	HSPA8	IL2RB	PICALM	SLC22A5	KCNJ6	SLC12A4	GP1BB
FOXO1	SOX10	KREMEN1	FGF23	USF1	ADCY6	CNGB1	ADRA1D
SOX9	ITGB4	CAMK2G	SIK2	AP2S1	VAC14	DPP6	SNCAIP
WWOX	STS	MECP2	DGCR8	NRF1	RAD23A	DLG3	HCRTR1
CYP1A1	MYLK	SPHK2	WNK1	TRIM21	LOXL4	STK24	P2RX3
IRF1	PTPN1	PFN1	NOG	PTGER3	EIF3F	PDE4C	NDUFB10
KLF6	ANGPT2	HUWE1	KRT10	KRT13	DOCK6	MGAT2	BPGM
ATRIP	NCAM1	ARF6	BPTF	DCLK1	GBF1	VAPB	NDUFA1
FGFR4	CD4	CDK5	PVR	PRKAR1B	DARS1	ALG1	KCNQ4
CBFB	SFRP1	FTO	PAK6	SPG7	GRIN2B	NDUFS4	ARHGAP4
AXL	AIFM1	CKB	TNFRSF12A	GJB1	KPNA1	GPD2	P2RX4
ITCH	TRPS1	FZD3	TRPM8	CD5	CRY1	MYH3	AQP2
PHB2	XRCC4	CSTA	HYOU1	PTS	CSTB	C1R	KMO
KLK3	TXN	SELE	CTRC	SIRT5	ERAP1	CACNA1B	PON3
CXCL8	DCK	PRDX6	HELLS	MAPKAPK3	AIMP1	PLOD3	ALS2
AKT2	ILK	TRPC4	CST3	TNFSF13B	ADCY3	LRP8	SERPINI1
STAG2	HLA-G	CYP2C9	TARDBP	PDHB	RAB11A	SLC27A2	RASGRP2

BRCA2	AURKB	AMACR	IRF8	CUL2	PGM3	UGT8	SLC26A3
IGFBP3	TYR	SMURF2	FSHB	WNT10A	SLC6A4	ACAN	ACAT2
DNMT1	TNFRSF11A	GSR	COL4A1	SH3GL1	HERC2	MID1	PGAM2
SOX2	CDH13	ATG5	PARN	PTGDS	CTH	ZIC1	ALDH4A1
ZEB1	B2M	PRKCQ	RFC1	HTRA1	LTB4R	VDAC3	CLCN2
CTSD	MSLN	ITGB2	LAMB3	KAT8	RNASEH2A	NT5C3A	CACNA1I
SMAD2	CSNK2A1	NSUN2	LMNB1	ITGB5	HDAC11	TUBB4A	DPP10
PRLR	LRP6	POU2F1	AKR1B10	PDHX	DIAPH1	UQCRFS1	ALAS1
TCF7L2	KCNQ1	PRKD1	FZD1	POLR3B	PLCB3	EN2	KCNC3
ERCC1	TUBB	ACVR1	CLTC	SEMA3C	MSX1	SLC1A3	TPH2
CEBPA	ADAM17	LAMC2	GC	HDC	PUS1	GNAL	SYNJ1
RARB	DDX5	TWIST2	CD247	ADORA2A	MOGS	MYT1L	SPR
TBX3	ABCC3	TRIM25	ELN	ACAT1	TNFRSF21	OPRD1	KCNC4
CCND2	TGM2	MATK	EEF1A2	SLC16A7	MYOCD	ALAS2	KCNJ10
VDR	SYP	PRMT5	SRF	H6PD	NSDHL	GNAT2	AGA
DNMT3A	CADM1	CSF3R	IREB2	NIN	GRK5	NDUFS1	IL5RA
LEP	TKT	LAMP1	OFD1	POLL	GALNT3	PNPT1	CHRM4
PLAU	TMEM43	UMPS	EPHB3	MAN1B1	STXBP2	SLC22A2	OXCT1
PDGFRB	DUSP1	MCM4	EFNB1	AGTR2	DSC3	SLC22A4	CSRP3
SETD2	PRKAA1	CCR6	SERPINH1	KLK1	NEK1	CFD	ZIC3
PCNA	FOSL1	SLIT2	EPHB1	GRIA3	CYP11B2	SNAP23	ABCA5
ROS1	AKR1C3	TFE3	ID2	EMD	MKNK1	DTYMK	KCNE1
IFNG	VTN	MALT1	RPL35A	TRPV1	LONP1	ADRA2C	FMO3
NKX2-1	TCF3	CDK8	RPA2	OTX2	CANT1	ADRA1B	CACNB4
TWIST1	IKBKG	CYSLTR1	DHCR7	PRIM1	IL23R	GNAT1	CLCN4
AXIN1	IL15	CIB1	PTPN2	NCF4	PADI4	CNTN1	RORB
CTLA4	IL6R	MMP15	TPT1	TNFRSF18	CHRM3	SORD	AGXT
CDK1	CDC25B	STIM1	TPO	SMPD1	PPP2CB	STX4	DAGLA
KRT7	ITGA2	PSMB5	HADHA	UNC13D	FERMT3	WNK4	CLCNKB
FLT4	CD80	TERF2	HNRNPD	SPI1	NOS1	ZIC2	ACAD8
CASP10	GPX1	FKBP5	SOD3	KNG1	TCIRG1	ADRB1	CPN1
FHIT	MCM3	MYH14	CD2	IL9	ASL	ALDH3A2	COX15
NAT2	DAPK1	NFIB	MYOD1	METAP2	FBLN5	STXBP1	NCAN
SP1	GATA1	FGF13	ERN1	SLC11A2	FECH	RPS6KA4	SLC22A12
RIPK1	CEACAM3	SFRP4	CDA	PDE4D	MAP3K12	NPR2	KCNE3
AKT3	CYP2E1	HSD17B3	GSK3A	IL2RG	SCO2	MTM1	ADRA2B
TOP2A	TLR9	PRKCZ	PLCB4	GANAB	GRIN2D	PRKG2	GP9
LDLR	WNT3	EIF3A	DFFA	TBX5	ICAM2	PDE4B	MYH2
GSK3B	MYBPC3	PPP1R1B	ATIC	TLR1	SLC26A4	PSTPIP1	GALM
CACNA2D1	ADAM12	MPL	EIF4A3	RPS6KA2	DOCK2	CARD9	BST1
KEAP1	ST14	FABP5	ACO2	MS4A1	GARS1	CYP51A1	PTGIR
BSCL2	EWSR1	CD19	SUV39H1	FOLR2	CDON	FGD4	SLC6A1
DCC	HSP90AB1	PGRMC1	HCLS1	MBP	GRIN1	SLC1A4	GJA8
IRAK4	HSPA9	SMC1A	PTBP1	SLC7A7	PITX1	PPP3CC	SLC25A20

BRCA2	AURKB	AMACR	IRF8	CUL2	PGM3	UGT8	SLC26A3
PAH	HAVCR2	ITGAM	FER	RNF2	APOA2	BCAT2	ATP2A1
VEGFC	PTPRJ	TRIO	PPIA	APH1A	CTSC	GLDC	APOC2
E2F1	CXCR2	CDT1	COL4A2	RACGAP1	DHODH	CDK5R1	FCN3
PDCD1	LYN	SPINT2	KL	PCNT	ANXA6	PSENEN	TSPAN7
BCL2L1	PRMT1	YWHAQ	ABCC6	RUVBL2	ADCY9	DBI	SCN2A
JAK1	KLK6	IFI16	MAP2K7	PRKCH	ARPC1B	KCNE2	CTNS
RHOA	SCN5A	KDM3B	HSD11B2	ARG2	MFN1	CA1	ADAMTS10
EXT1	U2AF1	CSNK1A1	PSMA1	AQP1	ATXN1	TPSAB1	SLC13A5
HGF	SFN	PTPN13	ICOSLG	AHSG	CHL1	GPD1	GALE
HSP90AA1	ARNT	GLO1	AURKC	FBN2	MYL9	AQP7	HGD
CAV1	MTRR	ESRRG	VAV3	FLRT3	ADK	B3GAT3	PPP3R1
DROSHA	IL7	GAB2	SIRPA	EFEMP2	CNR2	NR1D1	F11
MMP1	HABP2	ALPP	GGT1	SCARB2	FAH	KIF1A	S1PR5
IL10	TNC	GABRA6	LMO2	FCGR2B	ACTA1	DBT	HBG2
SRD5A2	LIFR	TMPO	CYP21A2	TRAP1	ME2	NARS2	MCHR1
FGF2	MDC1	CCR1	SIRT7	ACVRL1	SURF1	GM2A	ENPP3
ENG	MECOM	ARHGAP26	PTK7	DOCK1	NEUROD1	CHN1	GABBR2
TNFSF10	MYH9	GFAP	HLA-DRA	ACTG1	VARS1	TSFM	SCO1
PTK2	PRKAG2	SLC7A5	TLR5	ATP2C1	UBE2D2	CNTNAP2	CASQ1
MMP14	TRAF3	TAB1	PAX3	PABPN1	IRF9	RCAN1	NLGN1
NSD1	COL1A1	IFNGR2	PDHA1	USP10	GZMA	YARS1	CYP2U1
CYP1B1	WNT10B	PKN1	RAB27A	IRF5	LIPG	RDH5	SEPSECS
ABL1	MYD88	TRAF6	SOST	LAMP2	CSF2RB	CPB2	IL31RA
BMP6	DLL1	SMAD1	ASPH	ALDH1A2	CD3D	PPT1	LTC4S
CBL	TNNT2	GRM1	PNPLA6	GSTO1	CR1	POLR3F	HCN2
CEACAM5	NCL	GNGT1	APP	PIK3R4	UQCRC2	HTR1A	NPC1L1
TGFA	CD9	STK4	BCL11A	REN	GBE1	NDUFV2	CLCN5
CD82	ANGPT1	COL18A1	MAP3K11	PIK3R5	GCK	PROC	NPHS1
CSF3	APOD	SRSF1	SEMA4D	NR2C2	DUOX2	APBA2	GJB3
STAT1	HAS2	IRF2	PSAP	DDX1	POU3F2	SLC11A1	PTH2R
RELA	SLC16A1	MTHFD1	P4HB	LAMA1	PKD2	ADAMTS4	ACTN2
SNAI1	SHMT1	VASP	UBA2	ALDH3A1	SYT1	APOH	GRAP2
HDAC1	KAT7	FOXP2	TAGLN	VAMP2	TPP1	UGP2	GATM
HNF1B	SDC1	VAV1	NTF4	TOP3A	PRTN3	MMP20	COX10
NQO1	RRM2	LRRK2	USP8	EIF2AK4	FA2H	HADH	GRM2
PRF1	SERPINA1	EDNRB	EGLN3	ANK3	PTGES3	PI4K2A	GK
MCL1	DIABLO	EDN3	ULK1	F2RL3	PPOX	IL17RA	CA14
CASP9	APOE	NSD2	SEMA3E	NECTIN2	PSMC3	COL9A1	SGCD
ERCC6	IQGAP1	RHO	ORAI1	GHSR	PRKCSH	AGL	CACNG2
CXCL12	LCK	CA12	CAPN2	ALPL	GNPAT	KCNA4	GABRG3
BUB1	PKP2	TF	MMP16	CRYAB	POLA1	ADD1	P2RX2
DSP	MAP3K8	IKZF1	LAMA2	DYRK2	CD209	KPNA3	MEGF10
NME1	PIM1	SPRY4	ARRB2	LCT	SERPINF2	RNASEH1	UPB1

BRCA2	AURKB	AMACR	IRF8	CUL2	PGM3	UGT8	SLC26A3
MAPK3	NGF	CRAT	ASAH1	TDP1	CA4	MMAB	GALR3
PRKCA	PTPN6	ADAM10	TACR1	FZD6	HSPA2	CTSZ	SLC1A1
ATP7B	CDH5	INPPL1	NIPBL	KCNN4	NLGN3	CLCN6	UMOD
ACTC1	INHBA	CALM1	FGF14	KCNMA1	EIF2B2	ASIC2	SLC18A1
ZFHX3	CLDN1	MMUT	PPAT	CASK	MAP3K3	DLX5	SLC6A19
ETV6	SUZ12	HP	RPS6KA5	PTPRN2	DDOST	NPR1	GABRA2
AHR	LIF	PRKCI	ITPR3	AIRE	ABCG1	CETP	MYBPC1
NPM1	GJB2	UGCG	CD74	SORL1	IVD	RHOT1	SGCG
MAPK10	NGFR	NNMT	TNKS	LTBP4	PIP4K2A	TOR1A	SCN2B
DPYD	CD46	GNB3	GCLC	EZH1	CHSY1	ROBO3	PLN
EFNA3	CUBN	UBE2C	GP1BA	HRH2	MARS1	RPE65	DGKD
FOXO3	CSK	TACC3	WNT11	SLC22A1	HSD17B10	NAGA	TPH1
PTGFR	TNFAIP3	PKD1	PLA2G6	FGF12	PSMD2	DRD1	MYL4
FN1	RELB	ABCC5	DYRK1A	ANP32A	NAE1	RHAG	GPR37
MAPK8	CD8A	FOXL2	TLR7	ACTN1	PRODH	ITPA	GABRB3
TPM1	IL6ST	XDH	PTGER2	IL11RA	GAA	SCN3B	GYG1
OGG1	PLA2G2A	PTGER4	CLDN18	TGM1	PDXK	AOX1	GRIA2
SNAI2	CARM1	SOX5	CX3CR1	A2M	COPB2	MLYCD	KERA
TRIM24	EDNRA	CD79A	GART	C5AR1	PRKAG1	DNAH11	ENTPD2
COMT	GRN	HTR2C	SIRT2	CHRNB4	HTR3A	SUCLG1	SLC7A9
VIM	PTPRD	ST3GAL1	CD14	NR4A3	CDH15	LCP2	GAMT
TP73	SERPINB2	USP9X	MAPKAP1	MATR3	P2RY1	SLC12A7	CYP4F2
IGF2R	CYP3A5	PRDM1	PAX2	NLRP1	MYLK2	GCGR	PDHA2
RARA	HSF1	NME2	ABCA3	APTX	PYCR2	C1QB	GABRR1
NFKBIA	TGFB3	C3AR1	HGFAC	TBX21	ZYX	DNAJB2	KCNN2
SNCG	CTBP1	TNFRSF4	MCM6	COL4A3	MED23	CYP7B1	ATP6V1B1
STAT5A	EIF2AK3	FLNB	FZD4	CSF2RA	MCCC1	LMAN1	SLC6A13
CCND3	CCNA1	CXADR	AGPAT2	C4A	PSMA6	SLC19A3	GLRB
ZEB2	MYO7A	YWHAZ	CD22	KIF2A	ELOVL5	MTNR1B	GRIN2C
TOP1	EHMT2	RPL11	EFNB2	CA8	PSMA5	HMOX2	GABRA5
ODC1	NRP2	KCNJ4	ST6GAL1	ARHGEF1	GALC	TEC	IL1RAPL1
MYH11	NHERF1	NDUFA13	ORC1	IFIH1	SRPK2	PGM1	APOA5
TYMP	NT5E	NUP214	MSX2	SATB2	CRYAA	ADD3	KCNC1
EPHB2	ATF3	BMPR1B	IMPDH2	USP14	LRAT	TXK	SLC26A5
SLC2A1	VCAN	KDM6B	CR2	RCC1	P4HA1	CLEC7A	CA5A
SERPINE1	WNT4	SH2B3	ALDH1A3	SULT2B1	TANK	SLC6A5	P2RY11
MAPK14	MIF	AGT	STAR	CPOX	CD33	BLVRA	CHRNA6
SOS1	PLAT	THRA	SAMHD1	AOC3	PDE8B	CAPN3	SLC32A1
PIK3CD	TFDP1	SLC2A4	TALDO1	P2RY2	TYROBP	CARTPT	GABRB1
PPP2R1B	SPHK1	DLK1	SENP1	ABCA7	PLIN1	RPIA	SLC1A6
RBBP8	SKP1	CPT1A	PRKG1	DLAT	GRK3	DDC	PRSS12
PPP2R2A	TK1	NAA10	SIAH1	FZD9	PLOD2	ABAT	P2RX1
RPS6KB1	HDAC3	EGLN1	CYB5A	ACE2	ALPI	SARDH	SLC9A6

BRCA2	AURKB	AMACR	IRF8	CUL2	PGM3	UGT8	SLC26A3
CSF1R	GMNN	SERPINA3	PRKD2	PAK5	HMGCS2	SLC39A8	GYS2
ICAM1	DDIT3	FABP4	HNRNPH1	TRPV4	RBP4	SLC12A6	HTR1F
FOS	HSP90B1	PRDX1	TLN1	GCG	PIGA	CHMP4B	DCX
BIRC3	GPI	ALOX12	TRPV6	POLR1A	ITGA7	UQCRC1	KCNT1
FOXM1	FGF17	KDM5C	PNKP	MGLL	CYP46A1	CTSA	SLC18A3
RAC1	TIAM1	DAG1	USP1	FXN	DPEP1	COX6B1	NPY2R
CTCF	LIG1	SETDB1	LMNB2	MARK4	AGPS	DARS2	HCN4
EPHB4	PTPN12	GNE	SFPQ	APLNR	NLRC4	DLG4	SLC22A6
RRAS2	NEK9	ACP5	JAG2	CAPN1	LARS2	DUOX1	MSMO1
RPS20	TRIM28	PCBP1	TBP	SMAD5	RAPGEF3	SLC12A5	GLRA2
MAP2K2	AMPH	TMPRSS6	ANXA11	GUCY2D	RNMT	NDUFA6	CELA2A
DNMT3B	CTSK	CBLB	GAL	SQLE	MYO9B	CBLIF	KCNJ8
INSR	FUS	COL1A2	P2RX7	ALDOB	EXTL3	GRM4	
CASR	ROCK1	SEMA4A	COL17A1	SI	SLC4A1	AMPD3	
PTHLH	ACTN4	ABCB11	CANX	G6PC1	SV2A	OCRL	
SPP1	CUL3	DNASE1	HAX1	CACNA1D	GALT	PIP5K1C	
SKP2	APAF1	CD79B	RPS3	C3	STT3B	PLAA	
POLK	G6PD	CNTFR	ZBTB16	EEF2K	ADORA3	BTD	
PRL	FOXP1	ATF2	CLOCK	PDK4	FARSB	VPS35	
PLK1	FGF9	AHCY	OCA2	DDX6	GABRA3	DGKA	
IRS1	MAP3K7	CTSS	F7	GUCY2C	CALCRL	C4B	
ABCC4	ITGA5	HSPB8	MEFV	SERPINB6	SERPINA6	ENO3	
PIK3R2	HES1	CCKBR	GPT	TREX1	KCNA5	ABCC8	
CCNB1	IGFBP4	DVL2	MYO5A	CCKAR	GNB5	CLCN3	
ACTB	LTA	CDC45	ATP2A2	COQ8A	SEC63	ASIC1	
PKM	HLA-DRB1	DNAJB1	RELN	FXR1	CIT	TARS2	
PLAUR	MAF	RPL5	ATF6	SDC2	NFIA	TRPC3	
FASN	FOXC1	DUSP3	RPN1	SYNGAP1	D2HGDH	SLC5A7	
TNFRSF10B	HLA-DQB1	CD58	KDM4A	COMP	LFNG	DGAT1	
NOTCH2	CXCL10	TRIM33	MCM5	IL21	CFB	PNLIP	
MC1R	CDC20	RAD23B	RPS17	PSMD14	GOLGA2	ATP6V0C	
SLC19A1	MAD2L1	ANO1	PEPD	BDKRB2	PTPRN	ACADVL	
PDGFB	ADH1B	TUBG1	AKR1A1	GFPT1	KIF22	NRXN3	
XIAP	IL13	GLB1	RPL10A	CASP4	OPTN	NKX2-5	
TIMP1	F2R	BUB3	CAMKK2	ITIH4	MAN2B1	ACADSB	
TGFBR3	CTSE	RPS14	IHH	WARS1	UFD1	SLC16A2	
TGFB2	RASA1	APOA1	ZAP70	PSMA3	GNMT	ARL3	
CFTR	RPSA	RPS19	SIAH2	FLNC	UCP1	HMGCL	
APEX1	OSM	PSAT1	RNF168	TUBA1C	PNPO	TTBK2	
CYLD	SLC25A15	LIG3	GBA1	ITGA2B	FCGRT	NPY1R	
KRT5	HNF4A	IL17RD	PRKCG	CLPB	KIF5A	FBXO7	
PTPN3	GPX4	USP15	EFNA5	ARF1	CHKB	DBH	
MED1	HMGCR	MAP3K14	FES	DSG1	SLC25A3	ABCD1	

BRCA2	AURKB	AMACR	IRF8	CUL2	PGM3	UGT8	SLC26A3
FGF3	GRB7	S1PR2	TRPM7	CCR4	APOC3	GNS	
CYP2D6	BTK	RIT1	FCGR2A	DPAGT1	VARS2	NEFH	
AREG	SMARCA2	LGR5	PABPC1	ARHGDIA	UCHL3	SLC29A2	
NOTCH3	ATF1	MINPP1	MAT2A	ENDOG	SLC5A2	GIPR	
MMP7	CD276	TPM2	DPM1	EMX2	DMP1	KCND3	
TSHR	CAST	VIPR1	MAP3K2	PPP2R2B	PRSS3	NCS1	
HSPB1	TERF1	GUSB	PMEL	ACSF3	PPP3CA	KCNK1	
PAK1	PDGFA	TAP1	BGN	HIF1AN	LITAF	SYCP3	
HDAC4	SSTR2	RPL26	TPM3	EPS8	PIK3C2B	ADCY7	
KRT8	CYP2C19	YES1	DLL3	NRG2	PTPRZ1	ACTG2	
SOCS1	CDH23	KDM5A	SKI	DCTN1	CNTN2	M6PR	
FBN1	IFNB1	CHD4	PLD2	CLCN7	GDI1	NDUFV1	
KDM4B	BTRC	RANBP2	C1QBP	ASPA	MPDZ	TNNT1	
CDKN2C	TNFRSF9	CD27	ITK	TXN2	GRIK3	PDE2A	
CREB1	GZMB	TFPI	NHEJ1	EYA1	PDE4A	LPA	
HMGA2	CCR5	RUVBL1	MYO6	MEF2D	VDAC2	GCNT2	
CYCS	GH1	CD63	MIB1	CLIP1	EIF2B4	KIRREL3	
PIK3CB	RARS1	NR2F1	ABCB4	NUP62	PHKG2	GRM3	
KRT18	MAPT	TTN	COL2A1	ARSA	LRP4	MASP2	
COL3A1	LHCGR	IL3RA	IL12B	BMP5	TFR2	PMPCB	
CCNA2	CYP27B1	FKBP1A	TBXT	PSMC1	GDF11	GDAP1	
CDH3	SSTR1	GAPDHS	KCNH1	DPP9	NPPB	SLC2A10	
MDM4	TJP1	MAPK11	ITPR1	BNIP3L	ATP1B1	SERPIND1	
IL4	MSN	CUL4A	LAMB1	NCF1	DNM3	PCYT2	
KLF4	SRGAP1	TIE1	PRNP	PYY	PDCD6IP	PDE6B	
CSF1	SEMA3A	KLK4	MAOA	PPP2R5D	TAT	NRXN1	
LEPR	MYL3	CIC	GRB10	SLCO1B3	ALDH18A1	NDUFB9	
TIMP3	RBBP4	BCL2L2	MAPK13	TREM1	BLK	IRAK3	
DDR1	DOT1L	FUT8	ASNS	COPA	NDUFS8	AP1B1	
E2F4	WNT3A	CHRNA5	SRPK1	SCP2	GFER	ATP13A2	
BAK1	S100A8	IL12RB1	SPTBN1	SLC25A11	OLR1	GMPPB	
GRB2	SRD5A1	RPA1	PSMA7	TFAM	SIGMAR1	ADAMTS5	
CSF2	DCN	CISH	TACR3	DLST	B3GAT1	HLCS	
ACTA2	CCNE2	FOSB	RPL35	FADS1	FHL1	XYLT2	
CDC25A	RHEB	MMP17	GGPS1	NR4A2	ADORA2B	GRIA4	
TLR4	NUMA1	GABRB2	ABCB5	TH	ALG8	SLC14A1	
BMI1	NR4A1	NEDD4	IRAK1	LNPEP	SUCLA2	ACOX2	
XBP1	L1CAM	SIN3A	PTPRA	DCLRE1C	DNAJC6	SLC6A2	
KITLG	RBL2	PARP2	LAMA3	CRBN	B4GALT1	PYGM	
STAT5B	MAPK9	POR	NT5C2	CYP2R1	LHX3	PICK1	
PPP2R1A	CD55	SLC6A9	PROS1	NPC1	UBE2A	RGS10	
MYB	CSNK1D	ADNP	ITGAL	NFATC3	COASY	GFM1	
CCL2	PXDN	RDX	PDGFD	DYSF	NLRP2	ADRA2A	

BRCA2	AURKB	AMACR	IRF8	CUL2	PGM3	UGT8	SLC26A3
PRKACA	TNNI3	EEF1A1	PRPS1	MFAP5	ARX	BACE1	
INS	VCAM1	COL11A1	EPRS1	PPIF	EIF2S3	NFASC	
ETS1	POLB	PIM2	PRKAR2B	HAMP	AK1	CHRNE	
THBS1	CD47	AMHR2	ENPP1	CD2AP	GSS	DGUOK	
EPHA2	RBX1	LRP5	SCARB1	CALM2	CMA1	GJA5	
WNT5A	MYL2	SLC13A3	PNP	AQP3	SERPING1	NDUFS6	
DSG2	CXCR3	CAD	INPP5D	PAK3	FIBP	TBXA2R	
POU5F1	SLC1A5	NECTIN4	SLC16A3	ADCY8	YARS2	SCN10A	
NOS2	PSEN2	KAT6B	CX3CL1	NCF2	DGKZ	DGAT2	
NCOR2	IGFBP7	HPN	NR1H4	SLCO2B1	CPT2	PRCP	
MTR	GLS	ENTPD3	RASGRP1	EFNA4	CFI	TREM2	
BMP4	CUL4B	NUP98	ADAMTS1	MDH1	IL21R	RARS2	
SHH	ROR2	PRKACB	TCL1A	PFKM	ATP2B2	COQ7	
REST	SLC5A5	SIRT3	EIF4B	GNB4	PDYN	TRPA1	
PML	CHI3L1	THPO	SSTR3	FTL	KCNQ5	HARS1	
FLT3	CD86	VWF	NOX4	PANK2	CAMK2A	CRADD	
AGO2	ADA	PKD2L1	FBL	ITGB7	SNRPN	EPX	
LEF1	CCR2	ITGA4	POLI	CACNA1C	SEC24C	ABHD5	
MED12	PGK1	UCHL1	BLNK	SLC40A1	PMM2	PZP	
MME	CCK	TFG	WAS	ITM2B	MAPKAPK5	NGLY1	
SERPINB5	CD59	PRSS8	TAF1	SLC29A3	NNT	PANX1	
PTK6	AFP	VIP	IFNGR1	LPIN1	TAOK1	KCNJ11	
CDH2	EPHA1	IL5	TAL1	PTPRU	GCH1	ENTPD5	
PTK2B	TTK	PARK7	STAT2	ADRB3	PDE3A	SARS2	
ALDH1A1	GLI3	EIF5A	PAX7	TNFRSF13C	LCAT	CNGA1	
SIRT1	UBE2I	PRDX5	FZR1	RTN4	PYGL	FCER2	
LDHA	GFRA3	PRKAA2	SLC6A3	COL5A2	PMPCA	PHYH	

Supplementary Table 4: Docking scores of Sitogluside to high scoring hub gens in PPI network using Dockthor online tool.

Rank	File ID	Ligand-Receptor	Affinity	Total Energy	vdW Energy	Elec. Energy
1	e40d8dea56	Sitogluside-STAT3	-9.092	492.643	-23.017	-13.051
1	bb0d8fba57	Sitogluside-SRC	-7.935	493.097	-17.279	-19.131
1	fbc798577c	Sitogluside-MAPK1	-8.400	491.778	-19.483	-18.958